Structural Design of an High Speed Motor Yacht in GRP by Rules and direct FEM analysis

Marko Katalinić

Master Thesis

presented in partial fulfillment
of the requirements for the double degree:
"Advanced Master in Naval Architecture" conferred by University of Liege
"Master of Sciences in Applied Mechanics, specialization in Hydrodynamics, Energetics and Propulsion" conferred by Ecole Centrale de Nantes

developed at University of Genoa
in framework of the

"EMSHIP"

Erasmus Mundus Master Course

in "Integrated Advanced Ship Design"

Ref.

Supervisor: Prof. Dario Boote, University de Genoa

Reviewer: West Pomeranian University of Technology, Szczecin

Genoa, February 2012

Declaration of Authorship

I declare that this thesis and the work presented in it are my own and have been generated by me as the result of my own original research.

Where I have consulted the published work of others, this is always clearly attributed.

Where I have quoted from the work of others, the source is always given. With the exception of such quotations, this thesis is entirely my own work.

I have acknowledged all main sources of help.

This thesis contains no material that has been submitted previously, in whole or in part, for the award of any other academic degree or diploma.

I cede copyright of the thesis in favour of the University of Genoa.

Date: *Signature:*

13.2.2012. *Marko Katalinić*

Table of Contents

Table of figures

ABSTRACT

The thesis is developed during an industrial internship in a specialized composite shipyard. The aim of the thesis was to develop a high speed motor yacht, able to reach a top speed of 55 knots, based on a proven design of a fast patrol vessel. The reference project is a 13.2 meter planning hull made of FRP (Fiber Reinforced Plastic) with propulsion consisting of two diesel engines (600HP) driving two waterjets and allows achieving a top speed of 45 knots. The high speed motor yacht is 13.5 meters in length with propulsion consisting of two diesel engines (820 HP) driving two surface-piercing propellers. The work included interior and exterior design of the vessel and structural calculations of the hull, while always having in mind its influence on the hydrodynamics effects encountered at such a high speed.

The esthetical design and the general arrangement are defined in accordance with the top speed of the yacht that gives a baseline for its use, aiming at younger clients for weekend cruises, or to be used as a tender next to a larger yacht.

Structural design of the hull was performed using RINA (Registro Italiano Navale) FPV (Fast Patrol Vessel) and HSC (High Speed Craft) Code. The hull is made from a vinyl ester composite. Single skin laminate with glass reinforcement is used in the bottom area to absorb the high loads. The sides of the hull are in sandwich construction with glass reinforced skins and balsa core to be lightweight and stiff. Stiffeners have a polyurethane core and are reinforced with hybrid glass-carbon and unitape carbon fiber. As composite materials are tailored and customized to the needs of a specific project they offer a great potential to optimize weight and cost. Optimization was performed in an iterative manner for each hull panel and stiffener laminate layout.

Special consideration during the structural design of the hull was given to the transom. As opposed to the waterjet configuration the thrust loads from the surface-piercing propellers are absorbed by the transom. For that reason a FEM analysis of the transom was performed using ANSYS Structural software. The simulation was done in accordance with the complexity of the problem of modeling composite parts.

1 INTRODUCTION

The presented thesis is in a form of a design report. The aim was to develop a high speed motor yacht, able to reach a top speed of 55 knots, based on a proven design of a fast patrol vessel.

The reference project is a 13.2 meter planning hull specifically designed for patrol duties. It is made of FRP (Fiber Reinforced Plastic) with standard propulsion consisting of two diesel engines (600HP) driving two waterjets (Rolls-Royce Kamewa) and allows achieving a top speed of 45 knots.

To achieve the goals of the project it was necessary to rethink the following:

- General arrangement and Exterior design,
- Hydrodynamics and Propulsion,
- Structural design.

The top speed of the yacht, 55knots, gives a baseline for its use, aiming at younger clients for weekend cruises, or to be used as a tender next to a larger yacht. It also sets a compromise on comfort in reference to other yachts of the same length. The top speed, the aim of the use of the yacht, and its aggressiveness set a design philosophy to be followed in all parts of the design.

2 GENERAL ARRANGEMENT AND EXTERIOR DESIGN

Naval architecture and shipbuilding are very old and complex areas of man's interest. As such there is a lot of knowledge and experience acquired and contained in the work done throughout the ages. Although, each designer is aiming to contribute with something new and creative, it is common sense to use that which is already "discovered" and suits him. In line with this logic the first step of a new project is to a market research and to determine what are the latest standards set for the vessel type of interest and what is the market's heading.

As stated, a reference project has been chosen. It is a fast patrol vessel able to reach 45 knots top speed. It is a planning mono-hull hull form typical of offshore racing powerboats. Its service use and top speed give it an aggressive character and the exterior lines of the superstructure are in line with it. The profile view is presented in the following figure:

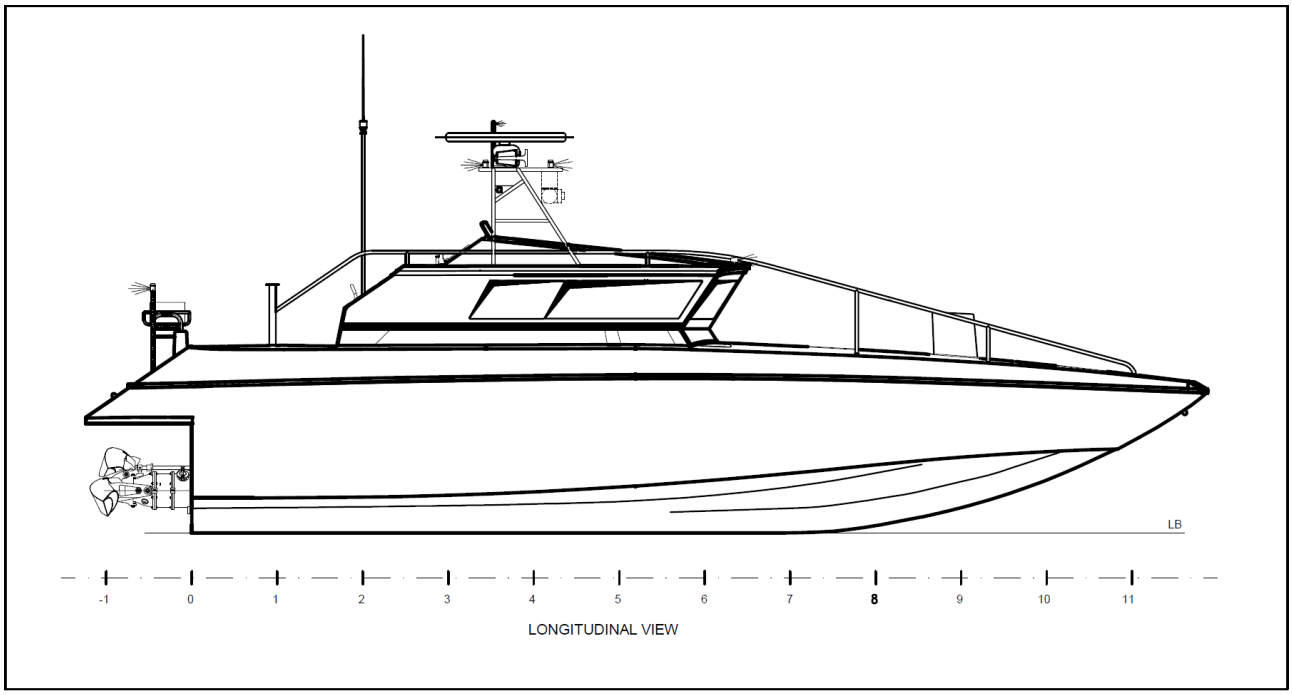

Figure 1. Profile view - reference project

This reference project was used as a starting point for the high-speed yacht project. Extremely high top speed which implies bigger engines (more noise and vibrations) and a change in propulsion type to surface piercing propellers (SPP), which offer a "water show" behind the vessel, very much emphasize the aggressively of the design overall. Thus it is necessary that the exterior lines follow the same logic to provide an adequate esthetic appearance.

After considering the possible options the yacht was defined to be of the „open type“ meaning that it does not have closed superstructure, but just a large windshield for riding comfort and protection. Also a part of the deck in front of the windshield has been elevated to ensure more space inside.

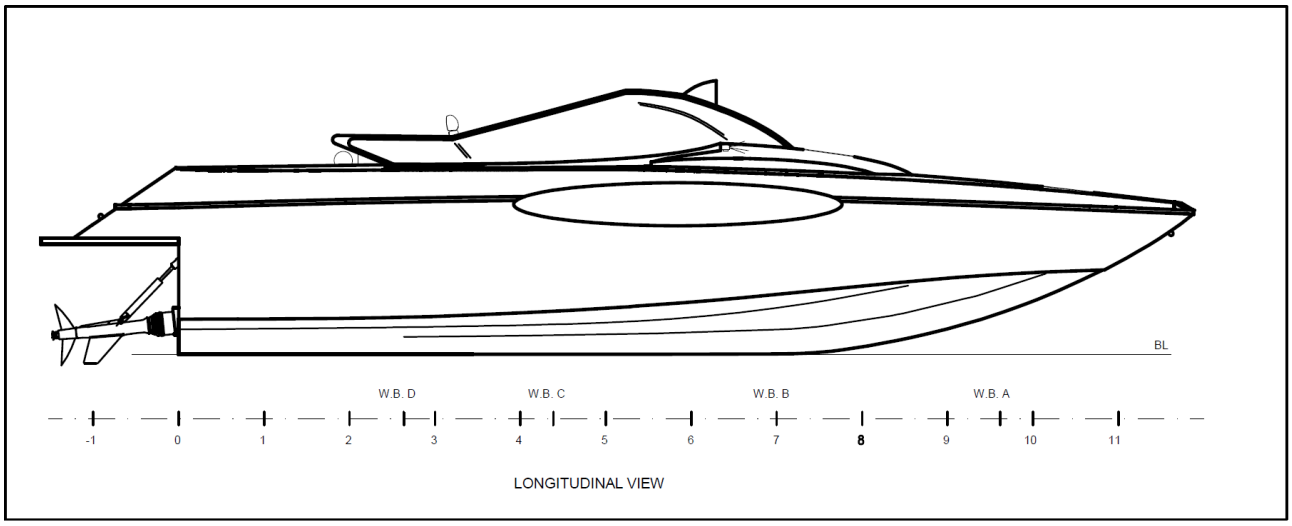

Figure 2. Profile of high speed yacht

The following figure presents a top view of the yacht indicating two main outside areas, a centrally placed cockpit and a sunbathing are with a little kitchenette in the aft. It can also be noted that the stern platform is grilled to provide unobstructed airflow to the SPP.

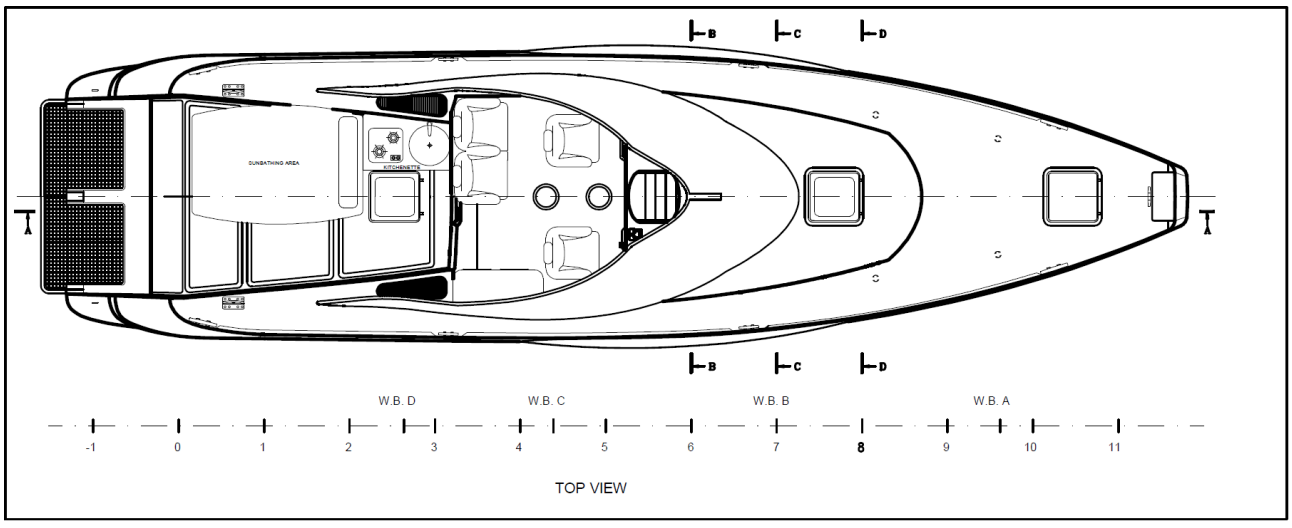

Figure 3. Top view of the high speed yacht

The following drawing presents a longitudinal section of the vessel and its main compartments.

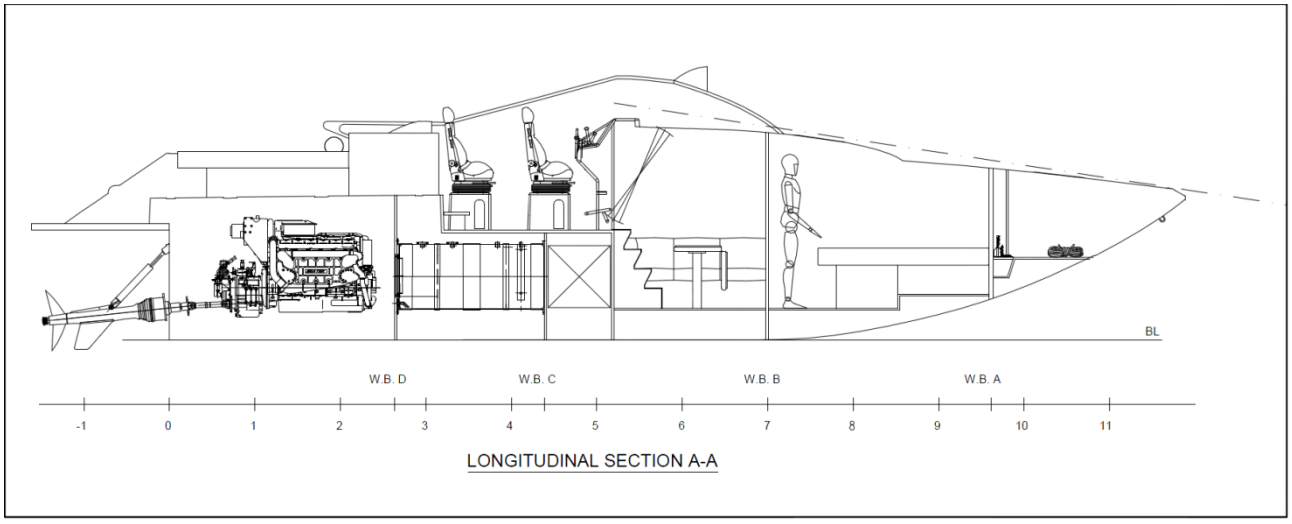

Figure 4. Longitudinl section of the vessel

From aft forwards the compartments are: engine room, fuel tank, water tank, inside living quarters with table and seating, toilet, navigation desk, and finally the bedroom with the king-size bed with a large storage space below.

The living quarters are shown in more detail in the following sections:

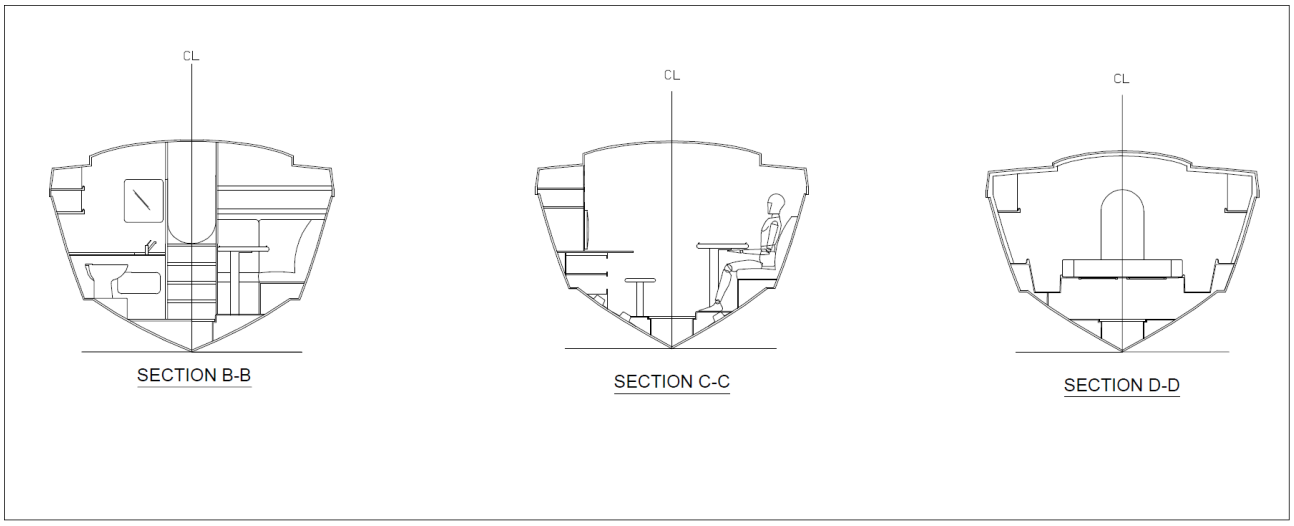

Figure 5. Living quarters sections

For more details, also a below deck plan is provided in the following drawing.

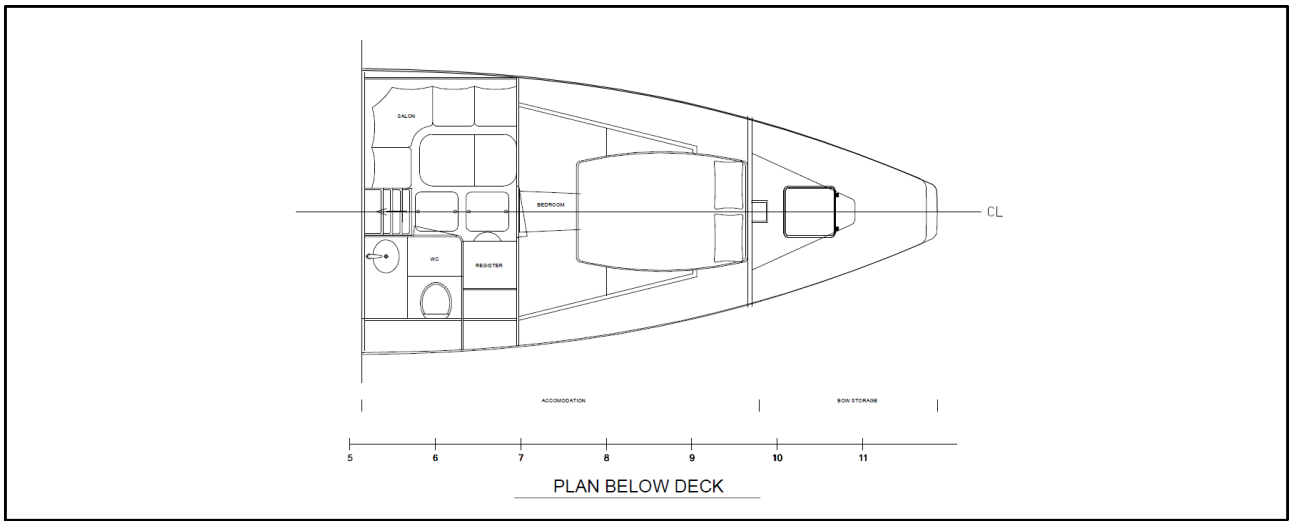

Figure 6. Plan below deck

Apart from the 2D drawing a 3D model has been generated to better demonstrate the general arrangement and the esthetics of the vessel. The model has been generated using Rhinoceros NURBS modeling software.

Figure 7. High speed motor yacht 3D model

The windshield design is as double-curvature multi-layered tinted glass enclosed with a stainless steel pipe. The front part of the windshield is very low profile to minimize air drag which can be substantial at the desired top speed, while backwards it ends in a sharp manner

re-evoking retro style lines as could be seen in the car industry during the sixties. This experiment has been done to avoid the “sad look” with a simple linear finish of the windshield profile. The windshield profile going “up” at the end ensures a dynamic look which is in line with the design philosophy of the yacht.

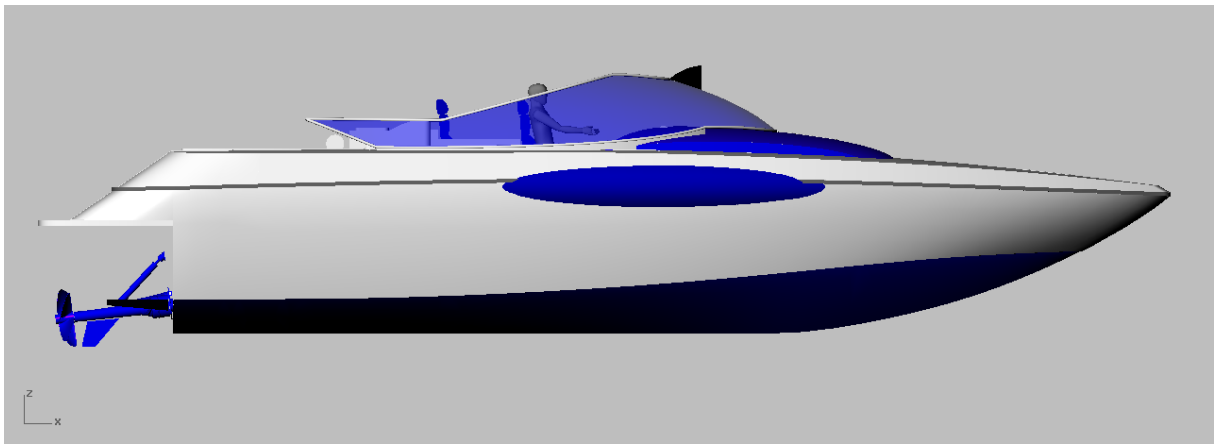

Figure 8. 3D model profile view rendering

The elevated part of the deck in front of the windshield, painted in blue on the following figure, in the service of the esthetical design provides a ‘dampening element’ between the deck angle and the windshield angle longitudinally. It also follows tangentially the curvature of the side „bumper“ (also painted blue).

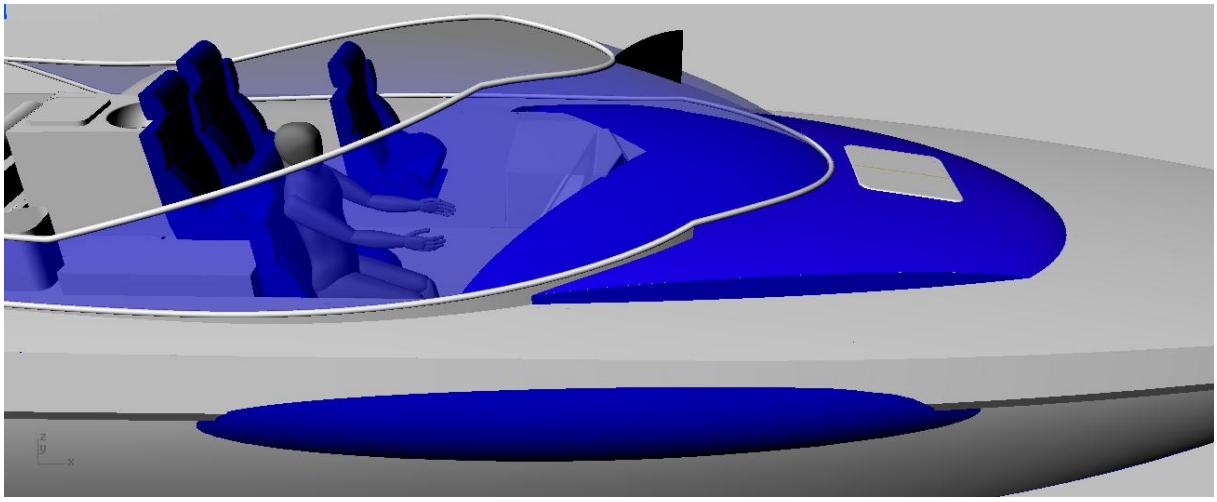

Figure 9. 3D model central part rendering

The bumper is semi-elliptic inflatable tube, as in standard RIB boats, to make docking easier and to avoid using a lot of movable bumpers so less people can more easily manage the vessel.

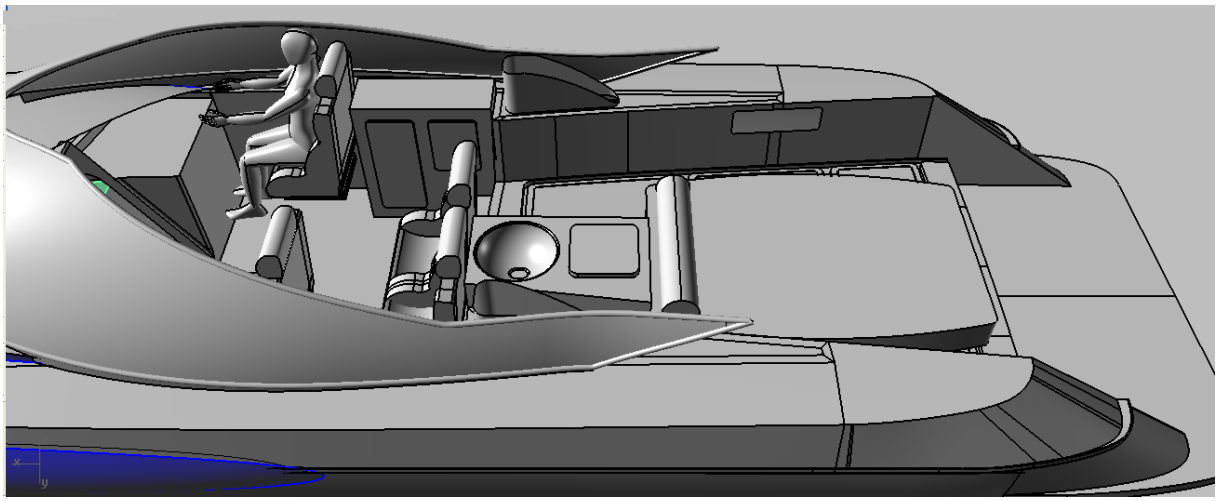

Figure 10. 3D model – Cockpit and sunbathing area

The cockpit is intended for seating the 4 passengers during navigation. Very high speed can cause high accelerations in rough seas, but also in calm sea conditions while encountering a wave from another boat. For this reason the seats should be equipped with belts and have their own damping system to ensure more pleasant frequencies to the passengers. While at anchor or in port the passengers can use the sunbathing area, the kitchenette behind the seats and a large platform for sea access.

3 HYDRODYNAMICS AND PROPULSION

3.1 Savitsky method

As previously stated, this project is performance orientated and the desired top speed of 55 knots imposed compromises to be made on other design aspects in terms of engine and fuel tank power and size, weight distribution etc. The preliminary resistance evaluation and behavior for a high speed craft (*Fn* = 6.2), i.e. a planning hull, can be done using the Savitsky method [7].

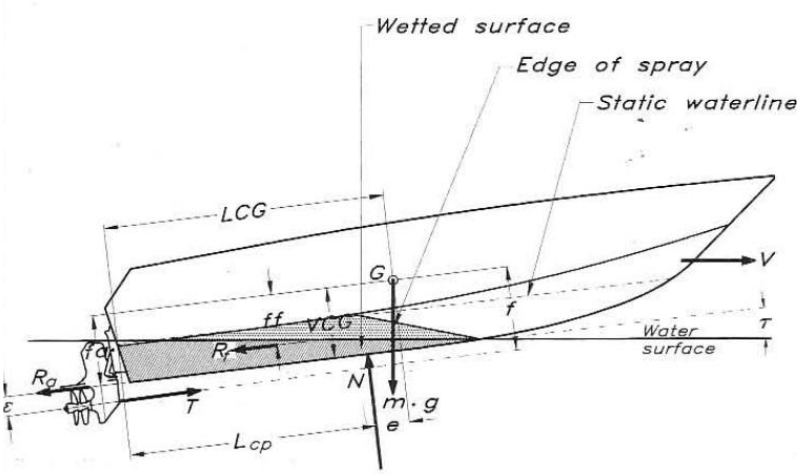

Figure 11. Forces acting on a planing hull by Savitsky

Daniel Savitsky was the first to scientifically approach the problem of planning hull dynamics and has set up a model to resolve the equilibrium of the governing forces.

Based on the Savitsky method the resistance force and power and trim diagram were calculated. Although it is a simplified method it is a valuable tool for preliminary assessment. For definitive conclusions more advanced CFD methods and towing tank testing are available.

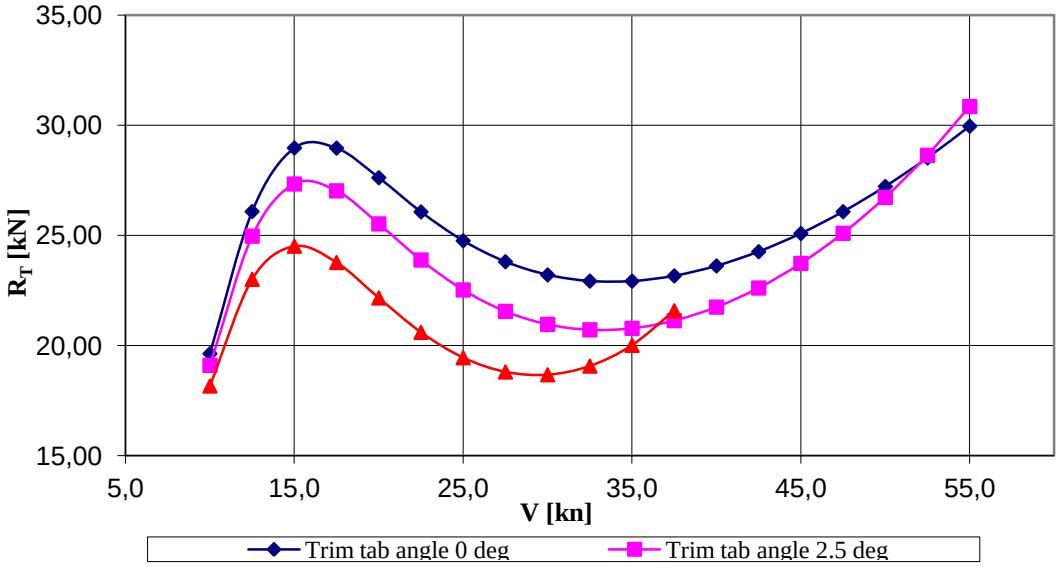

Figure 12. Total resistance force R_T / Speed diagram

Resistance force and power curves were calculated for different trim tab angles (0°, 4° and 12° respectively). Trim tabs are movable surfaces, usually hinged on the transom that can be used to decrease the angle of the vessel, their effect being proportional to the angle of rotation.

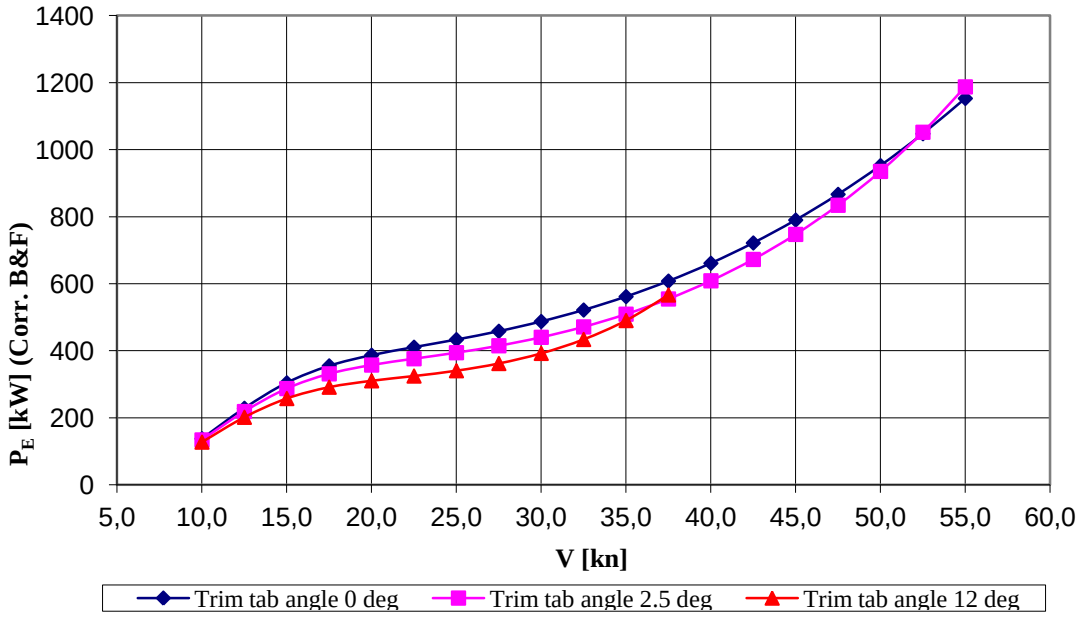

Figure 13. Effective power P_E / Speed diagram

It can be noted that the trim tabs play a significant role on the resistance of a planning vessel. Resistance can be decreased if the vessel operator uses a higher trim tab angle (ex: 12 deg) when the vessel is in the pre-planning regime (from 10 – 35 knots) and decreasing it afterwards. Higher trim angle in the pre-planning regime will decrease the over exaggerated trim of the vessel (figure bellow) thus reducing the pressure resistance of the yacht.

It is worth mentioning that Savitsky found that the optimal trim angle to aim for, for the minimal total of pressure and friction resistance equals around 4°, where frictional resistance grows rapidly with small trim angles and pressure resistance with high trim angles.

Another hydrodynamic consideration needed to be taken into account was the prevention of porposing. Porpoising is a phenomenon of dynamic longitudinal instability of the hull making it impossible to achieve a stable running trim. It is characterized by an oscillation combination of heave and pitch even in clam water conditions. It depends on various factors but mostly on the position of the center of gravity of the vessel and the position of the center of the dynamic pressure on the bottom, and can be influenced by many hull features.
According to the Savitsky method and based on the hull parameters a critical trim angle can be calculated to define a stable, non porposing regime.

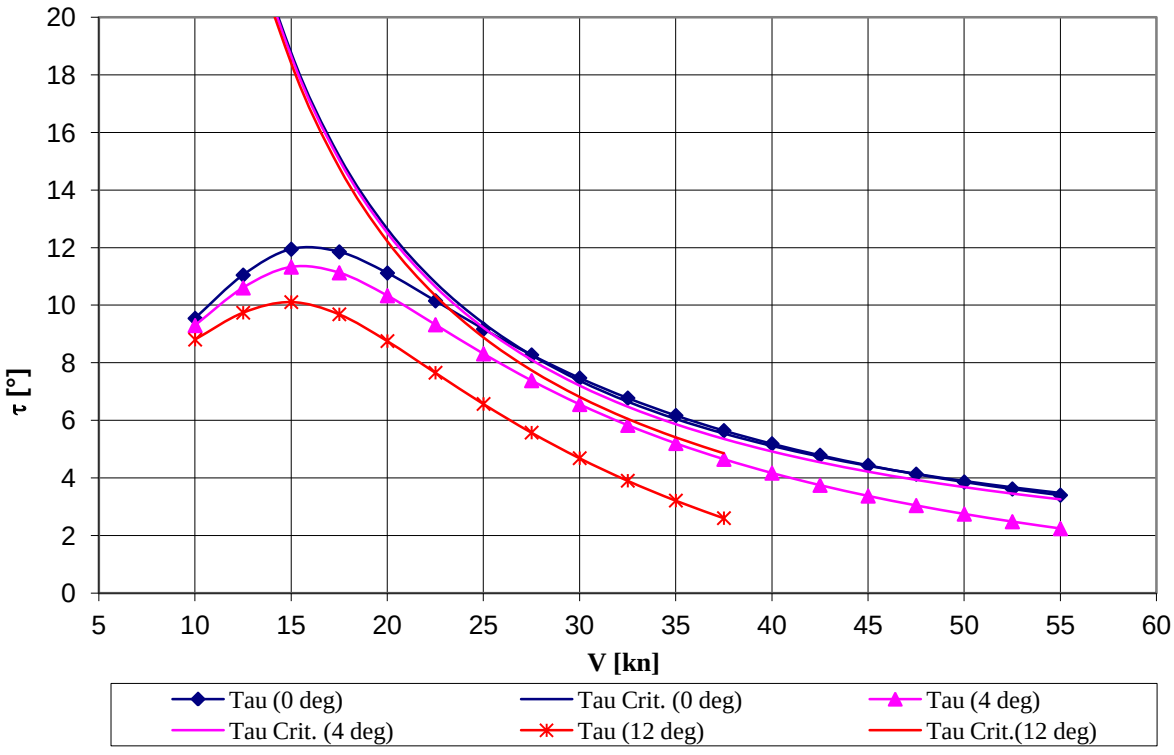

Figure 14. Trim diagram

It can be seen that with the trim tabs angle equal to 0° the yacht is in the limit state to experience porpoising for the great part of the planning regime. This represents a serious problem for the yacht. The problem needs to be solved in a way not to alter the reference hull form, at least not in a major way, as it would require new moulds to be manufactured for the production and this would create a significant additional expense.
It is visible from the graph that the phenomenon can be controlled by the trim tabs for the great part of the planning regime as it is also advisable to reduce the resistance. But for top speed the trim of the vessel is too low to use trim tabs as it can lead to an increase in the frictional resistance component but, more important, it can be dangerous if the bow meets a wave in correspondence with the low trim as it can cause high deceleration forces or even capsizing in the longitudinal direction.

There are several ways to influence the porpoising problem:

- Using dynamically computer controlled trim tabs to correct the vessel's trim based on the acceleration data acquired from the gyroscopic sensor.
- Moving the center of gravity backwards to reduce the bow-down moment which arrives from coupling the weight G and the bottom pressure resultant N, as in figure 2.
- Prolonging the sprayrails backwards, if possible, to enclose the flow between them making the pressure area narrower and moving the center of pressure forwards, thus reducing the bow-down moment described in the previous point.

As for the power prediction, to achieve the top speed of 55 knots it was determined to use more powerful engines, namely two Seatek 820HP engines, and the waterjet propulsion system was replaced by Arnesson SPP (Surface-Piercing Propellers) drives.

The sum engine power is in accordance with the Savitsky resistance prediction with the overall propulsion efficiency coefficient (OPEC) equal to 0,7.

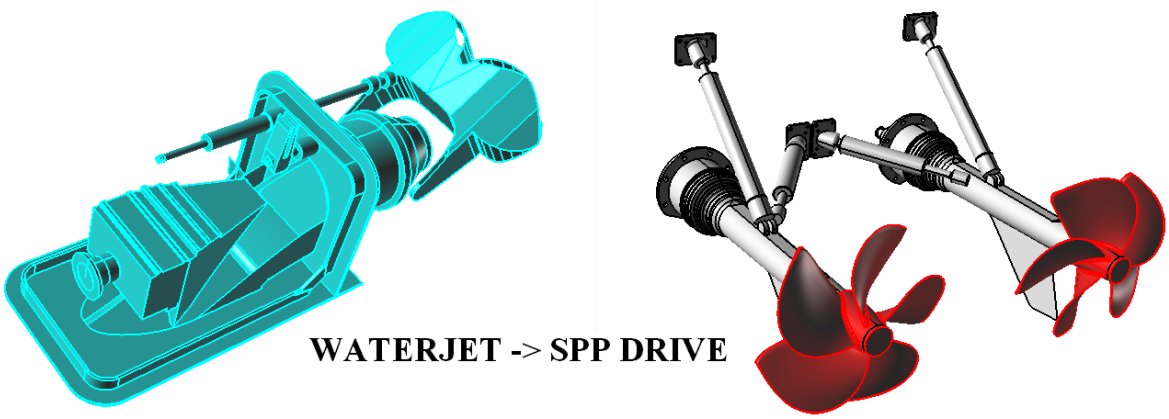

Figure 15. Waterjet and Arnesson SPP drive 3D models

The decision to change the propulsion type is based on several considerations. It generally has a better overall efficiency coefficient than waterjets for very high speeds. And, the use of the Arnesson SPP drive made possible to move the center of gravity backwards and to prolong the sprayrails backwards to prevent the porpoising problem. It requires less space in the engine room making it possible to shift the main engines, the fuel tanks and the engine room equipment backwards enough to achieve the desired weight shift. The sprayrailes could be prolonged backwards as there was no more limitation on their length as with the waterjet configuration where the waterjet intakes required unobstructed flow in front of them.

3.2 Surface piercing propellers general features

As aiming for higher speeds propulsion efficiency becomes more and more important. While conventional slow turning – large diameter propellers are the best choice for slower vessels, waterjet efficiency becomes better with larger *Fn* (Froude number) i.e. with higher speeds, and there are no problems with the appendages, and collision damages.

But when aiming for very high speeds and wanting to maximize efficiency to decrease the engine and fuel cost one can turn to the surface-piercing propeller, a solution well proven on racing boats.

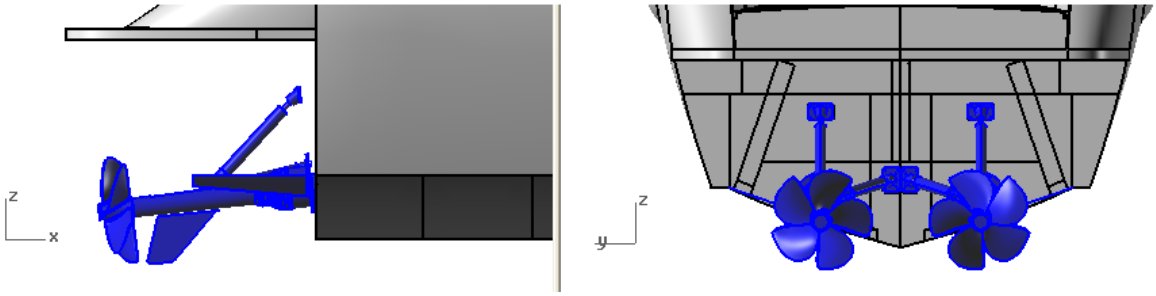

Figure 16. Arnesson surface piercing drive mounted on the stern

SPPs are usually placed behind the transom, with only a part of the propeller disk in the water. Its main advantage is the same as for the waterjet: no submerged appendages are needed. The shaft may stick directly out from the transom thus relaxing the restrictions on the propeller diameter thus increasing efficiency. Both super-cavitating and conventional blade sections are used, and since much air is entrained at the water impact of each blade the collapse of cavitation bubbles (now partly filled with air) is smoother. The main disadvantage of surface-piercing propellers is the large variation in blade loading. At the top position, when the blade is in the air, the loading is zero, while when the blade points downwards the loading reaches its maximum. Apart from generating vibrations, this pulsating load causes fatigue which needs to be considered in the design [1].

4 MATERIALS AND TECHNOLOGY

4.1 Composite materials in general

Composite materials (or shorter composites) are defined as homogenous material obtained by combining two or more different materials, filers or reinforcement with a compatible matrix as a bonding agent to obtain specific properties [2]. A special group of composite materials are fiber reinforced composites. This group has, in reference to other construction materials, certain advantages and disadvantages.

The most important advantages are:

- Significantly higher specific strength and rigidity in respect to low density
- Durability against the majority of acids and alkali
- Self-extinguishing and anti-corrosive properties
- High capability of vibration damping
- Low production costs

The biggest disadvantage is relatively high price of certain components, most of all reinforcements, which limits the area of use.

Composite properties are specific in reference to the properties of its components and represent more than a simple sum of the component properties. Consequently, it is necessary to insure good compatibility of the matrix and the reinforcement. In this manner it is possible to obtain a material of specific properties which none of the components have by itself. Thus, the properties of a composite depend on its components and their interaction in the finally shaped material.

When resin systems are combined with fiber reinforcement excellent properties can be obtained. The polymer matrix distributes the loads of the composite material in whole to each fiber and protects the fiber from abrasion and impacts. A result is a material of high strength and rigidity, low density and durable against atmospheric conditions.

In contrast to steel and aluminum, composite materials (e.g. glass reinforced plastic, shorter GRP) have the advantage of tailoring the material properties for each application. This results in lighter but stronger materials.

However, finding an optimum solution for the laminate requires sophisticated calculation methods, material evaluations and experience. The strength of the laminate is not a single-meaning value, it depends on the direction. To know the strength of the laminate it is necessary to know its lay-up where the most important parameter affecting the strength is the form of the reinforcement.

4.1.1 Reinforcement

Generally, there are three types of reinforcement fibers used, independently or combined, for manufacturing a composite material: glass, aramid (Kevlar, widely used commercial name) and carbon fibers.

In the boat building industry the most commonly used reinforcement type is the E-glass. Strength wise there may be better materials but when taking into consideration combined cost, strength and effectiveness the E-glass often remains the best choice.

Glass reinforcement is available in various forms:

- Chopped Strand Mat (CSM) – short fibers 4-5 cm of glass held together by a binder;
- Unidirectional Roving (UDR) – strands of fibers held together by a light stitching;
- Woven Roving (WR) – strands of fiber woven together (0°, 90°);
- Biaxial Roving (BR) – two layers of UDR (0°, 90°) held together by a light stitching;
- Triaxial Roving (TR) – three layers of UDR (0°, 45° and 90°) lightly stitched together;
- Rovi-Mat (RM) – WR, BR or TR sewn to a layer of CSM

One of the most common used types of reinforcement is chopped strand mat (CSM) which is an isotropic reinforcement type. Woven roving (WR) or Biaxial Roving (BR) have better properties in the directions of the fiber. Thus, it is a “good practice rule” to use WR (or BR) to take care of primary load directions and to ensure sufficient inter-laminar strength (strength between plies of reinforcement) with a layer of CSM between each roving layer.

4.1.2 Resin

There are three most important types of resin:

- Polyester resin,
- Vinyl-ester resin,
- Epoxy resin

Although all three resin types can be used in combination with glass reinforcement, the most often choice is polyester resin (ortho- or iso-) and sometimes vinyl-ester resin. Resin curing during a lamination manufacturing is a very delicate chemical process which often requires the control of temperature, pressure, humidity etc. to ensure the desired mechanical properties.

An important parameter regarding strength properties of the laminate is the fiber content, often expressed as a percentage by weight of the total laminate weight. Generally, the higher fiber content that can be reached the laminate becomes stronger, as long as the fibers are not subjected to resin starvation. In practice it is not realistic to count fiber content that higher than 37% and lower than 27% when using a wet hand lay-up with a mat laminate. With a mix of mats and woven rovings in the laminate the fiber content usually varies from 35% to 45% and with multidirectional material (rather than woven) up to 55%. These contents can be decreased with vacuum infusion or pre-preg methods.

4.1.3 Sandwiches

In addition to single skin laminates sandwich construction has been widely adopted in the boatbuilding industry. Building a yacht of sandwich construction offers the following advantages:

- It gives a light building weight. However, practical considerations mean that the outer skin cannot be made too thin or else there will be insufficient strength to withstand docking, grounding and boatyard handling. The weight advantages for sandwich construction are therefore not so apparent in yachts below cca. 9 m
- Sandwich construction is able to utilize a stiffener free construction, making the hull totally self-supporting, but in the case of building a boat of more than 7.5 m totally

self-supported by its own hull panels results in very high demands on the core material and skins.

- This method enables a boat to be built as a one-off where no moulds are available.

The greatest advantage with sandwich construction is the possibility to increase strength and stiffness without a corresponding increase in weight. E.g., by increasing the total thickness of the panel without increasing the total thickness of the laminates, the stiffness increases seven times for a doubling of the panel's thickness. As a core material to separate the two laminate skins various materials can be used like: PVC or PU foam, PC honeycomb, balsa wood etc.

The materials chosen to be used for this project, as well as their properties, are reported in the following pages:

4.2 Material properties

4.2.1 Vinyl ester resin

This type of resin is a thermoset polymer along with polyester and epoxy resin. It is, in fact, an epoxy – vinyl ester resin dissolved in styrene monomer. Vinyl ester resins are considered to be a relatively modern type and are characterized by high reactivity, good workability and are long-lasting. They insure high resistance to a wide spectrum of acids, alkali and solvents and show good dimensional stability at elevated temperatures [2].

By properties vinyl ester resins are considered to be between polyester and epoxy. They can be processed at room temperature and their chemical stability is on the same levels as epoxy.

An additional requirement for this specific project is that the resin should be adequate for the process of vacuum infusion, meaning low viscosity, to insure good flow through the laminate during the infusion of the hull shell with the longitudinal stiffeners. It is also advisable to choose a low "print through" resin for esthetic reasons during the lifetime of the vessel, but also to prevent osmosis.

4.2.2 Fiber reinforcement mechanical properties

Material:	**0/90° Glass 1225 kg/m^2**		(Shell)
	Tensile strength	480 MPa	
	Tensile Modulus	26900 MPa	
	Thickness	0.97 mm	
Material:	**± 45° Glass 1225 kg/m^2**		(Shell)
	Tensile Modulus	18000 MPa	
	Thickness	0.97 mm	
Material:	**MAT 450 kg/m^2**		
	Tensile strength	98 MPa	
	Tensile Modulus	8050 MPa	
	Thickness	1.13 mm (hand lay-up), 0.94 mm (infusion)	
Material:	**MAT 225 kg/m^2**		
	Tensile strength	98 MPa	
	Tensile Modulus	8050 MPa	
	Thickness	0.65 mm	
Material:	**+/- 45 Glass - Carbon hybrid 820 kg/m^2**		(Stiffeners)
	Shear Modulus	25000 MPa	
	Shear strength	230 MPa	
	Tensile Modulus	14000 MPa	
	Thickness	0.90 mm	
Material:	**UNITAPE Carbon 820 kg/m^2**		(Stiffener head)
	Tensile strength 1370 MPa		
	Tensile Modulus 87550 MPa		
	Thickness 1.00 mm		

4.2.3 Core

Material: **BALSA CORE 150 kg/m^3** (Sandwich core)

Tensile strength	13.1 MPa
Tensile Modulus	4070 MPa
Shear Strenght	2.98 MPa
Shear Modulus	159 MPa
Thickness	12.7 mm

4.3 Vacuum infusion

The use of composite materials in boatbuilding has brought a big change in the number of boats being produced and their characteristics. Research has continuously been made in the field of these materials and has resulted in advancements as in the materials themselves as well as in the area of composite material production technology. Three most used techniques in the boatbuilding industry, of laminating a composite part, can be pointed out[9]:

- Hand lay-up (also sometimes called Contact procedure)
- Vacuum infusion (also called Vacuum assisted resin transfer moulding)
- Pre-impregnated lay-up (also called Pre-preg).

Hand lay-up lamination is historically the one with which it has begun to produce fiberglass and is still used in a lot of shipyards. Even the shipyards that claim to use other, more modern, techniques, still have to use hand lay-up for some connections, details etc.
The other two techniques represent a more modern approach in building composite parts and offer a way to improve the physical/mechanical properties of the final product.

Pre-preg's are cloths of glass, carbon or aramid reinforcement which already contain (are soaked) the exact desired amount of resin and do not require hand lamination in the shipyard. They simply need to be put on the mould and then "put under vacuum" and heated to elevated temperatures to enable the resin to react.

The vacuum infusion on the other hand includes forcing a liquid catalyzed, low-viscosity resin into a reinforced mold through low pressure. A flexible, airtight vacuum bag covers the mold and acts as a counter mold. Feed tubes placed parallel, perpendicular, in a herringbone pattern or an oblique pattern, depending on the shape of the object, distribute resin throughout the reinforcement as the vacuum is applied [10].

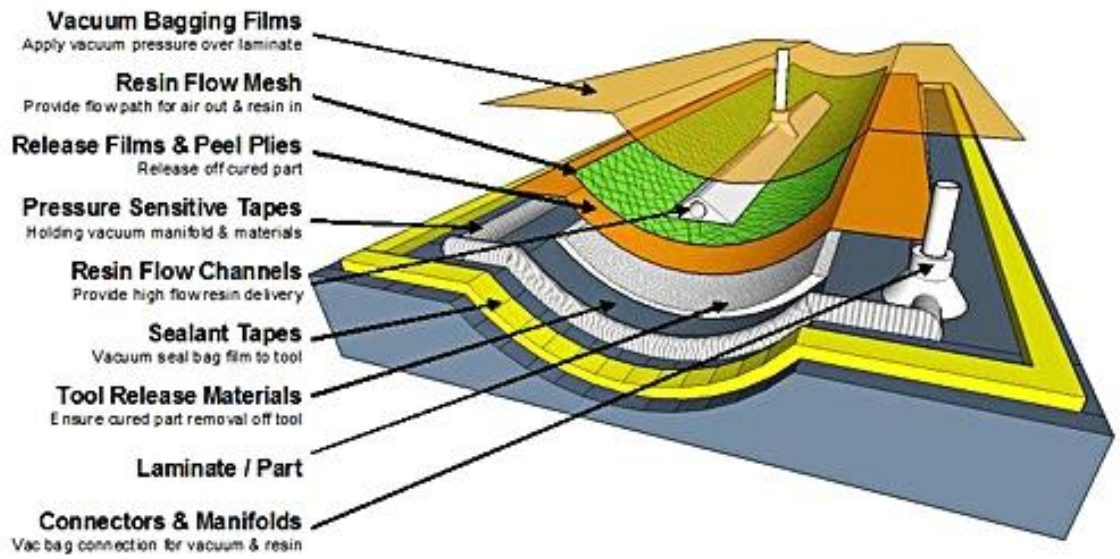

Figure 17. Vacuum infusion diagram. Available from http://www.tygavac.co.uk/process/resin-infusion.html

The benefits of resin infusion when compared to non-vacuum bag curing of composite laminates include:

- Better fiber to resin ratio
- Stronger laminate
- Low void content
- Reduces operator exposure to harmful emissions
- Reduced resin usage due to pre-compacted fabric
- Faster Ply lay-up

Typical wok-flow is demonstrated for a composite sandwich part:

- The mold is coated with a gelcoat layer
- Reinforcements and cores are placed
- The mold is covered with a flexible film
- Catalyzed resin is slowly injected
- Resin is sucked towards the vacuum pump and gradually fills the part. As a function of part size, catalytic conditions and type of core, injection pressure needs to be regulated
- Resin is sucked out of an open container
- Resin is distributed throughout the mold through a resin distribution network placed on the surface before the vacuum is applied. A grooved foam core performs the same function for sandwich materials
- Demoulding

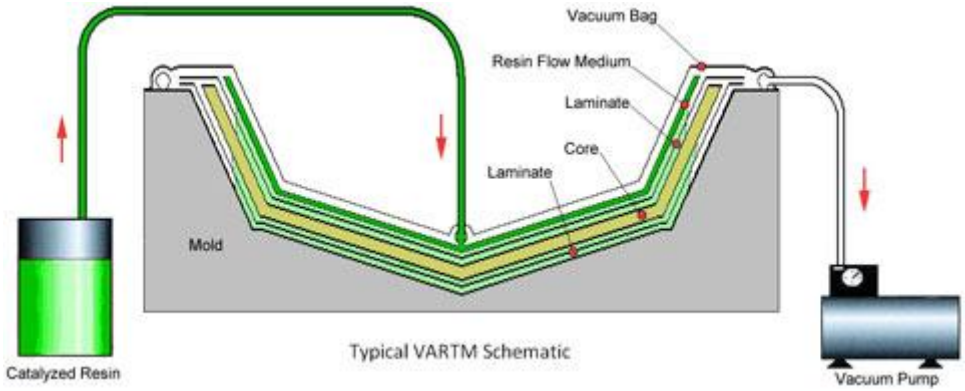

Figure 18. Infusion schematics.

Availale from http://www.energetxcomposites.com/vartm.html

5 SCANTLING BY RULES

Due to the very complex interactions between loads and strength requirements it is very difficult, by direct calculations, to determine the scantling of a vessel. For this reason different classification societies formulated scantling rules to follow in order to dimension a boat that will hold together if used as intended [1].

For the boat in consideration the RINA (Registro Italiano Navale) FPV (Fast Patrol Vessel) Code has been chosen. This code used is very similar and leaning to the RINA HSC (High Speed Craft) Code which is a logical choice considering the intended use of the boat. Structural members for the hull bottom and hull sides were studied and defined.

Te hull bottom is made from single-skin stiffened glass fiber, or hybrid glass/carbon, composite, while the sides are in balsa sandwich with skins in glass fiber. This type of construction results in a heavier but more flexible bottom which accounts for lower overall center of gravity hull with a bottom being able to withstand high loads from accelerations and slamming forces. At the same time the sandwich structure of the hull sides provides a stiffer, lower-weight, structure in respect to the single skin.

5.1.1 The structure of the RINA FPV code

RINA clearly states which loads are to be used, what material properties are to be considered and which safety factors are to be applied. The scantling requirements are based principally on strength requirements but also consider a serviceability issues, such as maximum deflection or minimum thickness of plates.

The scantling procedure for the vessel in consideration is based on local loading of panels and stiffeners arriving from the longitudinal distribution of vertical accelerations and impact pressure along the hull. As the vessel is built from composite materials that are highly customizable, and offer a possibility to optimize the material layout to save cost and weight, each panel and stiffener are examined separately adjusting its lamination scheme and schedule. The optimization of the lamination schedule was done in an iterative way using and automated MS Excel spreadsheet made for this purpose.

The scantling was determined in accordance to the following rules and procedures:

5.1.2 Main dimensions and definitions

According to:

FPV, Part B, Ch 1, Sec 2, SYMBOLS AND DEFINITION

[2.1.1] Definitions and symbols.

The definition of the main terms, symbols, and vessel parameters, applicable to the rest of the Code is defined as following:

Table 1 Main dimensions and definitions

L_{OA}	13,500	m	Lenght Overall
L_{WL}	10,289	m	Lenght of waterline measured with the craft at rest in calm water
L	10,289	m	Rule length, in m, equal to LWL
V	55,000	kn	Maximum service speed
T	0,740	m	Draught of the craft, in m, measured vertically on the transverse section at the middle of length L, from the moulded base line of the hull to the full load
Δ	10,700	t	Displacement
B_W	2,820	m	The greatest moulded breadth, in m, of the craft
B	3,350	m	The greatest moulded breadth, in m, measured on the waterline at draught T
t	4,000	°	Trim angle during navigation, in degrees, to be taken not less than 4°
a_{CG}	18,000	°	Deadrise angle, in degrees, at LCG, to be taken between 10° and 30°,
D	2,170	m	Depth, in m, measured vertically in the transverse section at the middle of length L from the moulded base line of the hull to the top of the deck beam at one side of the main deck
γ_{SW}	1,025	t/m3	Density of seawater
C_B	0,486	-	Total block coefficient (as per FPV.B.Ch 1.Sec 2 [2.1.1])

5.1.3 Scantling arrangement

The scantling procedure for this vessel is of local character, meaning that the vessel is examined panel by panel and stiffener by stiffener. This arrives from the definition of loads that are defined for each panel and stiffener separately depending on their geometrical characteristics, position, and some global parameters. First the panel and stiffener dimensions and geometrical characteristics were determined and identified. The scantling arrangement, panel and stiffener position spacing and span, was done based on the reference vessel accommodating the necessary changes. Adjustments were done in the machinery room (accommodating the new propulsion and leaving out details imposed by the old propulsion system), living spaces, and the requirement to shift the LCG as far aft as possible was always kept in mind.

5.2 Bottom plating

Hull bottom panels are identified in the following drawing:

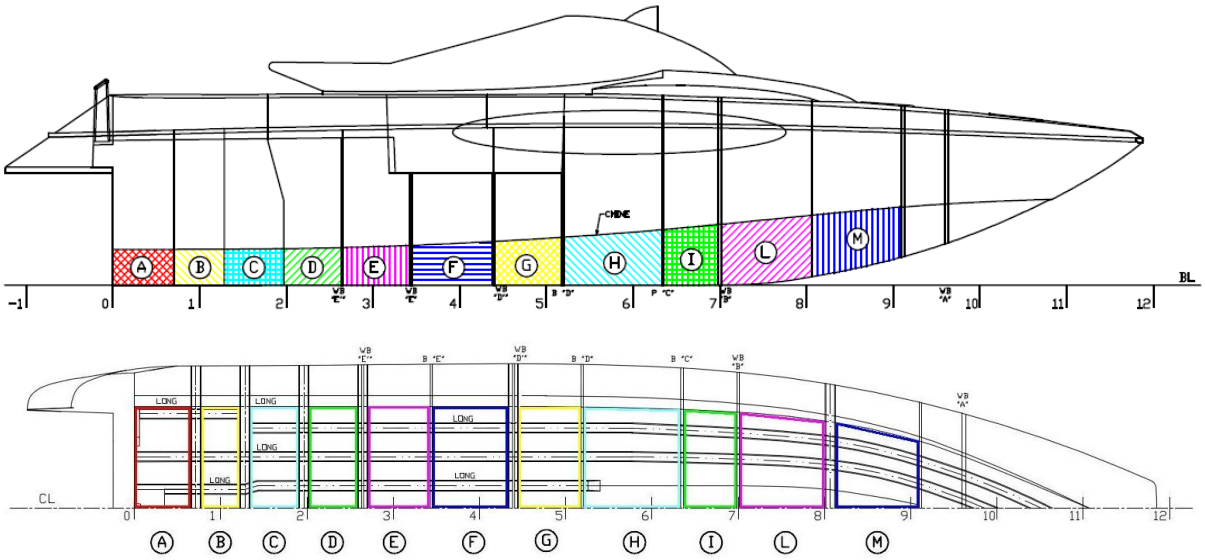

Figure 19. Panel identification - Hull bottom

The variation of the governing loads is dominant in the longitudinal direction along the hull, as will be seen later, and can be neglected transversally. Thus, neighbor-panels in the transversal direction are considered to be the same to simplify the calculation. The spacing

between the longitudinal stiffeners was defined in accordance with this, trying to keep the same or similar spacing – if possible in respect to the general arrangement. If the neighbor-panels in the transversal direction are not exactly the same, the largest is considered to be conservative.

Geometrical characteristics of hull bottom panels are defined in the following table:

Table 2. Geometrical characteristics of panels

PANEL	A	B	C	E	D	F	G	H	I	L	M
x [m]	0.346	0.978	1.628	2.335	3.064	3.894	4.817	5.768	6.665	7.515	8.617
αd [°]	19.150	19.334	19.430	19.820	20.600	21.940	23.890	26.880	30.000	30.000	30.000
s [m]	0.419	0.419	0.235	0.235	0.235	0.240	0.245	0.235	0.246	0.235	0.230
l [m]	0.652	0.452	0.565	0.610	0.668	0.938	0.668	1.131	0.636	1.042	1.042
x [m] - distance from AP to the center of the panel αd [°] - deadrise angle s [m] - spacing of stiffeners,measured along the plating l [m] - overall span of stiffeners											

5.2.1 Bottom single skin plating panel example

An example procedure of the bottom single skin plating panel A is presented. Geometrical characteristics of the example panel A are given in the following table:

Table 3. Geometrical characteristics of panel A

dist	0.346	m	Distance from AP
l	0.652	m	Overall span of stiffeners
s	0.419	m	Spacing of stiffeners, measured along the plating
αd	19.150	°	Deadrise angle
Z	0	m	Vertical distance from the molded base line to load point
f	0	m	Curvature offset of the shell plating

Loads and accelerations are calculated according to:

FPV Part B, Ch 5, Sec 2, [1] LOADS AND ACCELERATION

[1.1] VERTICAL ACCELERATION AT *LCG*

The design vertical acceleration, a_{CG} [g], corresponds to the average of the 1 percent highest accelerations in the most severe sea conditions expected, in addition to the gravity acceleration. It is to be not less than:

$$a_{CG} = foc \times Soc \times \frac{V}{L^{0,5}} = 7.314\ g \quad (1)$$

Where:

$foc = 1{,}333$ Type of service - Equivalent to maritime police - Table 1

$Soc(CF) = 0{,}320$ Unrestricted navigation - Hs > 4m - Table 2

Longitudinal distribution of vertical acceleration along the hull:

$$a_v = k_v \times a_{CG} \quad (2)$$

where ,

k_v Longitudinal distribution factor, depending on *x/L* (Part B.Ch 5.Sec 2 [1.1.4])

Thus, a diagram of the longitudinal distribution of vertical acceleration is obtained and will be applied, in an automatic manner using an MS Excel spreadsheet, in further calculations.

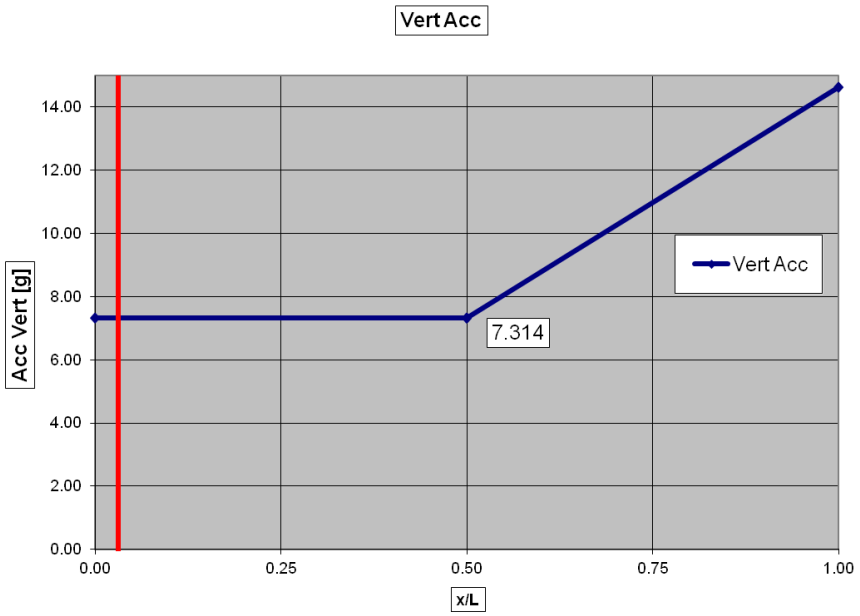

Figure 20. Longitudinal distribution of vertical acceleration

The increase of a_v towards the bow of the vessel is due to pitch effects. Variation of a_v in the transverse direction is generally disregarded.

Loads on the hull bottom are defined according to:

FPV Part B, Ch 5, Sec 2, [3], LOCAL LOADS [3.2.1]

The following loads are to be considered in determining scantlings of hull structures:

- Impact pressures due to slamming, if expected to occur,
- Sea pressures due to hydrostatic heads and wave loads,
- Internal loads.

Considering the type of the vessel, and following the design philosophy of a high speed craft able to withstand rough seas, the single skin bottom is dimensioned according to the impact slamming pressures which exceed the sea pressures due to hydrostatics and waves.

Loading point considerations are given according to:

[3.2.2] LOAD POINTS

Pressure on panels and strength members may be considered uniform and equal to the pressure at the following load points:

- For panels:
  - lower edge of the plate, for pressure due to hydrostatic head and wave load
  - geometrical centre of the panel, for impact pressure
- For strength members:
  - centre of the area supported by the element.

Impact pressure on the hull bottom is calculated according to:

[3.3.1] IMPACT PRESSURE ON THE HULL BOTTOM

Slamming expected to occur will induce the impact pressure, defined in kN/m2, considered as acting on the bottom of the hull and defined by the following formula:

$$p_{sl} = 70 \times \frac{\Delta}{S_r} \times K_1 \times K_2 \times K_3 \times a_{CG} = 141.2\ kN/m^2 \quad (3)$$

Where:

$S_r = 10.122\ m^2$ Reference area (as per FPV.B.Ch 5.Sec 2 [3.3.1])

$K_1 = 0.534$ Longitudinal bottom impact pressure distribution factor, defined as:

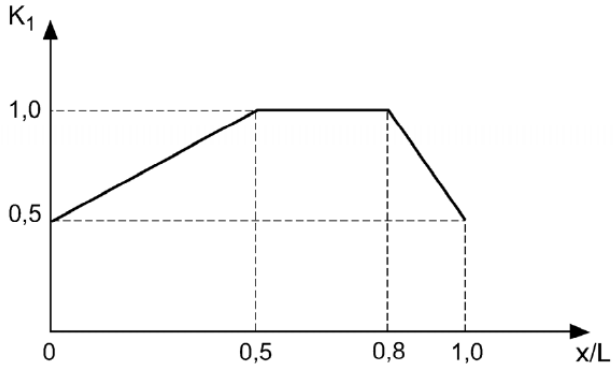

Figure 21. Longitudinal bottom impact pressure distribution factor

$K_2 = 0.5$ (calculated 0.418) Factor accounting for impact area, (as per FPV.B.Ch 5.Sec 2 [3.3.1])

$K_3 = 0.978$ Factor accounting for shape and deadrise of the hull, (as per FPV.B.Ch 5.Sec 2 [3.3.1])

$\boldsymbol{\alpha}_{dCG}$ is the deadrise angle, in degrees, measured at *LCG* and $\boldsymbol{\alpha}_d$ is the deadrise angle, in degrees, between horizontal line and straight line joining the edges of respective area measured at the longitudinal position of the load point; values taken for $\boldsymbol{\alpha}_d$ and $\boldsymbol{\alpha}_{dCG}$ are to be between 10° and 30°.

$\alpha_d = 30°$ deadrise angle

$\alpha_{dCG} = 19.15°$ deadrise angle at *LCG* ($10° < \alpha_{dCG} < 30°$)

5.2.2 Lamination scheme and schedule of example panel A

The lamination scheme and schedule of every panel was determined iteratively to obtain locally a material with properties to satisfy the Rules and minimize cost and weight. Gelcoat and mat plies are not considered to be load carrying and are neglected at this stage.

Table 4. Panel A lamination scheme and schedule

PLY	MATERIAL	ti (mm)	Ei (MPa)
1	0/90 GLASS 1225	1.16	23000
2	0/90 GLASS 1225	1.16	23000
3	0/90 GLASS 1225	0.97	26900
4	0/90 GLASS 1225	0.97	26900
5	0/90 GLASS 1225	0.97	26900
6	+/-45 GLASS 1225	0.97	18000
7	+/-45 GLASS 1225	0.97	18000
8	+/-45 GLASS 1225	0.97	18000
9	0/90 GLASS 1225	0.97	26900
10	0/90 GLASS 1225	0.97	26900
11	0/90 GLASS 1225	0.97	26900

Equivalent laminate properties to be used in for the plating calculation are determined following the Rule guidelines described in:

FPV Part B, Ch 4, Sec 1 MATERIALS, [4] COMPOSITE STRUCTURE

[4.3.3] Single skin laminates

b) The equivalent tensile elasticity modulus E_{tot}, in N/mm^2, of the multi-layer laminate may be calculated by:

$$E_{tot} = \frac{\Sigma E_i \times t_i}{\Sigma t_i} = 23737\ N/mm^2 \quad (4)$$

where

E_i Young's modus of layer *i*, in N/mm^2, assumed to be known and experimentally verified. E_i is the lowest of the values in tension and compression.

t_i thickness, in mm, regardless of direction (as per Part B, 4, 1, [4.3.3] - a)

c) The distance of the neutral fiber of the multi-layer laminate is, in mm:

$$V = \frac{\Sigma E_i \times t_i \times z_i}{\Sigma E_i \times t_i} = 5.56\ mm \quad (5)$$

where

z_i distance, in mm, from the neutral fiber of layer *i* to and edge (regardless of direction) (as per Part B, 4, 1, [4.3.3] - a)

d) The flexural rigidity of the multi-layer laminate [*EI*], by millimeter of width, in Nmm^2/mm

$$(EI) = \Sigma\, E_i \times \left(\frac{t_i^3}{12} + t_i + d_i^2\right) = 2794611\ Nmm^2/mm \quad (6)$$

where

d_i Distances from the neutral fiber of each layer to the neutral fiber of the laminate, in mm (as per Part B, 4, 1, [4.3.3] - c)

e) The inertia of the multi-layer laminate, by millimeter of width, in mm^4/mm, is:

$$(I) = \Sigma \left(\frac{t_i^3}{12} + t_i + d_i^2\right) = 112.45\ mm^4/mm \quad (7)$$

f) The theoretical bending breaking strength of the multi-layer laminate σ_{br}, is, in N/mm^2:

$$\sigma_{br} = k \times \frac{(EI)}{(I)}((1-\mu_0)^2 \times 10^{-3} = 422.5\ N/mm^2 \quad (8)$$

where

$k = 17{,}0$ For laminates using polyester (here applied on vinyl ester) resin.

μ_0 Vacuum content, equal to 0, if there is no available information.

Scantling guidelines are given in:

FPV Part B, Ch 5, Sec 2, [3] PLATING AND STIFFENERS SCANTLING

[1.1.1] General

The thicknesses, in mm, of plating are not to be less than the minimum values given by:

$$1.35 \times L^{1/3} \geq 2.5 \quad (9)$$

Table 5. Minimum thickness (as per FPV.B.Ch 5.Sec 3 [1.1.1] - Table 1)

Material	number	t_i [mm]	t_{tot} [mm]
MAT 450	2	1.13	2.26
0/90 GLASS 1225	5	0.97	4.85
±45 GLASS 1225	3	0.97	2.91
0/90 GLASS 1225	3	0.97	2.91
total thickness (mm)			13.31
minimum thickness (mm)			6.76

Condition satisfied!

[1.1.2] SCANTLINGS

Plating, hull, deck, bulkhead and superstructure stiffeners scantlings, for steel, aluminum alloy and composite material shall comply with relevant formulae as shown below referring to

HSC Code Ch3 [C3.7.7] for steel, or aluminum alloy vessels and [C3.8] for vessels in composite.

As instructed above for scantling considerations it is also necessary to consult:

HSC Code 2002 Ch 3.8 Fiber-reinforced plastic craft

Single skin stiffened panel, according to the Rules [3.8.4.3], will be verified against the following requirements:

- Minimum thickens of the single skin laminate plating
- Bending stress due to the design pressure
- Bending deflection due to the design pressure

[C3.8.4.3] Single skin laminates

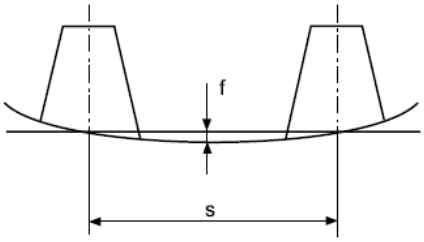

Figure 22. Bending of a single skin stiffened panel

.5 The bending stress, in N/mm2, due to the design pressure *p* is given by the formula:

$$\sigma_d = k_s \times \frac{V}{(I)} \times \frac{p \times s^2}{12} \times 10^3 \qquad (10)$$

where

ks	bending stress reduction factor	(as per HCS. Ch 3. 8. 4. 3. 1)
p	design pressure, due to slamming impact	(as per FPV.B.Ch 5.Sec 3 [3.3.1])
s	stiffener spacing as defined in Figure 22	

.7 The admissible bending stress σ_{de}, in N/mm2, calculated based on the theoretical bending breaking strength of the multi-layer laminate:

$$\sigma_{de} < \frac{\sigma_{br}}{SF} \qquad (11)$$

where

$SF = 4.5$ Safety factor (as defined in C3.8.4.2)

$$\sigma_d = 102\ MPa \quad < \quad \sigma_{de} = 106.7\ MPa$$

Condition satisfied!

The bending deflection, due to design pressure *p*, of a single-skin laminate between stiffeners is to be less than about 1% of the stiffener spacing. The bending deflection, in mm, of a single-skin laminate, fixed on its edges, is given by:

$$f = \frac{\mu_2}{384} \times \frac{p \times s^4}{(EI)} \times 10^9 \tag{12}$$

where

$\mu_2 = 0.9$ (as defined in C3.8.4.3.8)

$$f = 3.64\ mm \quad < \quad f_{max} = 4.19\ mm \tag{13}$$

Condition satisfied!

5.2.3 Bottom plating report

According to the procedure described above, following the same rules and steps, lamination scheme and schedule has been determined for all bottom panels and the results are summarized:

Table 6. Bottom plating scantling report

PANEL	A	B	C	E	D	F	G	H	I	L	M
x [m]	0.346	0.978	1.628	2.335	3.064	3.894	4.817	5.768	6.665	7.515	8.617
αd [°]	19.150	19.334	19.430	19.820	20.600	21.940	23.890	26.880	30.000	30.000	30.000
s [m]	0.419	0.419	0.235	0.235	0.235	0.240	0.245	0.235	0.246	0.235	0.230
l [m]	0.652	0.452	0.565	0.610	0.668	0.938	0.668	1.131	0.636	1.042	1.042
MAT 450	2	2	2	2	2	2	2	2	2	2	2
0/90 E 1225	5	4	4	4	4	4	4	4	4	4	4
±45 E1225	3	3	-	-	-	-	-	-	-	-	-
0/90 E 1225	3	3	3	3	3	4	4	4	4	4	3
thk tot	**13.31**	**12.15**	**9.05**	**9.05**	**9.05**	**10.02**	**10.2**	**10.2**	**10.2**	**10.2**	**9.05**
thk min	**6.76**	**6.76**	**6.76**	**6.76**	**6.76**	**6.76**	**6.67**	**6.67**	**6.67**	**6.67**	**6.67**
Etot	23737	23824	25786	25786	25786	25925	25925	25925	25925	25925	25786
V	5.56	4.97	3.4	3.4	3.4	3.88	3.88	3.88	3.88	3.88	3.4
EI	2.8E+06	2.1E+06	7.0E+05	7.0E+05	7.0E+05	1.0E+06	1.0E+06	1.0E+06	1.0E+06	1.0E+06	7.0E+05
I	112.45	80.62	26.09	26.09	26.09	38.94	38.94	38.94	38.94	38.94	26.09
K	17	17	17	17	17	17	17	17	17	17	17
σ_{BR}	422.5	433.3	480	480	480	480	480	480	480	480	480
Kv	1.000	1.000	1.000	1.000	1.000	1.000	1.000	1.210	1.296	1.461	1.675
av	7.314	7.314	7.314	7.314	7.314	7.314	7.314	8.200	9.476	10.684	12.251
S	0.273	0.189	0.133	0.143	0.157	0.225	0.164	0.266	0.156	0.245	0.24
u	2.699	1.871	1.312	1.416	1.551	2.224	1.617	2.626	1.546	2.419	2.368
K_1	0.534	0.595	0.658	0.727	0.798	0.878	0.968	1	1	1	0.906
K_2	0.500	0.5	0.512	0.502	0.5	0.5	0.5	0.5	0.5	0.5	0.5
K_3	0.978	0.974	0.973	0.965	0.95	0.924	0.887	0.829	0.769	0.769	0.76
p [kN/m^2]	**141.2**	**156.9**	**177.3**	**190.6**	**205.1**	**219.7**	**232.3**	**224.4**	**208.2**	**208.2**	**188.7**
μ_1	0.93	0.68	1	1	1	1	1	1	1	1	1
a	0.40	0.4	0.4	0.4	0.4	0.4	0.4	0.4	0.4	0.4	0.4
rc	1.00	1	1	1	1	1	1	1	1	1	1
ks	0.37	0.27	0.4	0.4	0.4	0.4	0.4	0.4	0.4	0.4	0.4
SF	4.5	4.5	4.5	4.5	4.5	4.5	4.5	4.5	4.5	4.5	4.5
σd	**102.0**	**38.6**	**42.5**	**45.7**	**49.1**	**42.0**	**46.3**	**41.2**	**41.8**	**38.2**	**43.3**
σde	**106.7**	**106.7**	**106.7**	**106.7**	**106.7**	**106.7**	**106.7**	**106.7**	**106.7**	**106.7**	**106.7**
μ2	0.90	0.55	1	1	1	1	1	1	1	1	1
f	**3.64**	**3.4**	**2.01**	**2.16**	**2.32**	**1.81**	**2.08**	**1.7**	**1.9**	**1.58**	**1.96**
fmax	**4.19**	**4.19**	**2.35**	**2.35**	**2.25**	**2.4**	**2.45**	**2.35**	**2.46**	**2.35**	**2.3**

5.3 Side plating

Hull side plating is made in sandwich construction. The pressures acting on the sides are expected to be less than the pressures acting on the bottom. This enables the use of sandwich construction which, in respect to a single skin laminate, ensures higher relative stiffness and reduced mass. The sandwich layout used is glass composite skins encapsulating a balsa core. Balsa core is chosen for being medium lightweight, applicable for vacuum infusion, and for being a natural material with good fire properties (does not create dangerous hazardous fumes while burning).

The hull side plating is divided into panels between the stiffeners in the same manner as for the bottom plating in the previous chapter. An example panel scantling calculation is given for Panel 1.

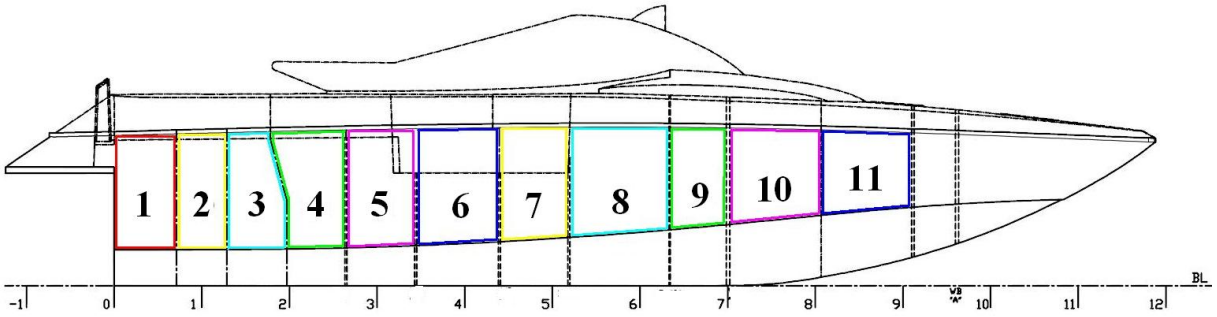

Figure 23. Hull side plating division

Table 7. Geometrical characteristics of side sandwich panels

PANEL	1	2	3	4	5	6	7	8	9	10	11
x[m]	0.325	1.018	1.6275	2.335	3.064	3.951	4.684	5.7675	6.665	7.515	8.617
αd [°]	19.150	19.334	19.430	19.820	20.600	21.940	23.890	26.880	30.000	30.000	30.000
s [m]	0.652	0.452	0.565	0.610	0.668	0.938	0.668	1.131	0.636	1.042	1.042
l [m]	1.295	1.382	1.390	1.398	1.394	1.394	1.375	1.275	1.196	1.097	0.969
Z [m]	1.065	1.07	1.078	1.09	1.107	1.131	1.16	1.196	1.231	1.263	1.294

x[m] - distance from AP to the center of the panel
αd [°] - deadrise angle
s [m] - spacing of stiffeners, measured along the plating
l [m] - overall span of stiffeners
Z [m] - Vertical distance from the moulded base line to load point

The core thickenss for all side panels is beforehand determined to be equal to 12.7 mm.

5.3.1 Hull side sandwich plating panel example – Panel 1

Table 8. Geometrical characteristics of example hull side sandwich panel 1

dist	0.346	m	Distance from AP
l	1.295	m	Overall span of stiffeners
s	0.652	m	Spacing of stiffeners, measured along the plating
αd	19.150	°	Deadrise angle
Z	1.065	m	Vertical distance from the molded base line to load point
f	0	m	Curvature offset of the shell plating

Main symbols and definitions defined in (FPV, Part B, Ch 1, Sec 2, [2.1.1]) and given in the beginning of the Scantling chapter in this report stay the same.

Also the vertical accelerations and their longitudinal distribution defined in (FPV, Part B, Ch 5, Sec 2, [1.1]) are the same as for the bottom plating calculation in the previous chapter.

As for the design pressure considered acting on the side shell, opposite from the bottom plating where the slamming impact pressure was considered, according to (Part B, Ch 5, Sec 2, [3.2.2]) the sea pressures, due to hydrostatics and waves, are considered and calculated as follows:

Sea pressures acting on the side shell are evaluated in accordance with:

FPV Part B, Ch 5, Sec 2, [4.1] Sea pressure on bottom and side shell

[4.1.1] The sea pressure, in kN/m2, considered as acting on the bottom and side shell is not less than p_{smin}, defined in the Table 7, nor less than:

for $z \leq T$:

$$p_s = 10 \times (T + 0.75 \times S - (1 - 0.25 \times \frac{S}{T}) \times z) \quad (14)$$

for $z > T$:

$$p_s = 10 \times (T + S - z) \quad (15)$$

where

z vertical distance, in m, from the moulded base line to load point. z is to be taken positively upwards

S as given, in m, in the following table with C_B taken not greater than 0.5

Table 9. Sea pressure definition

	S	p_{smin}
x/L ≥ 0,9	$T \leq 0,36 \cdot a_{CG} \cdot \frac{\sqrt{L}}{C_B} \leq 3,5 \cdot T$	$20 \leq \frac{L+75}{5} \leq 35$
x/L ≤ 0,5	$T \leq 0,60 \cdot a_{CG} \cdot \sqrt{L} \leq 2,5 \cdot T$	$10 \leq \frac{L+75}{10} \leq 20$

Between midship area and fore end (0,5 < x/L < 0.9) p_s varies in a linear way as follows:

$$p_s = p_{sFP} - \left(2.25 - 2.5 \times \frac{x}{L}\right) \times (p_{sFP} - p_{sM}) \quad (16)$$

where p_{sFP} is the sea pressure at fore end and p_{sM} in midship area.

For example Panel 1 it follows:

Parameter *S* and consequently the minimum pressure p_{smin} are calculated based on the longitudinal position on the vessel:

for	*x/L*>=0.9	*S*	=	2.59	m
for	*x/L*<=0.5	*S*	=	1.85	m
for	*x/L*>=0.9	p_{smin}	=	20	kN/m^2
for	*x/L*<=0.5	p_{smin}	=	10	kN/m^2

Sea pressure at fore end is calculated varying on the position of the center of the panel respect to the draught T, using the appropriate *S* (for *x/L*>=0.9).

for	$z<=T$	p_{sFP}	=	25.478 kN/m^2
for	$z>T$	p_{sFP}	=	22.520 kN/m^2

Sea pressure at midship is calculated varying on the position of the center of the panel respect to the draught T, using the appropriate *S* (for $x/L<=0.5$).

for	$z<=T$	p_{sM}	=	17.233 kN/m^2
for	$z>T$	p_{sM}	=	15.12 kN/m^2

Design pressures are extracted based on the vertical distance of the panel from the molded baseline to the center of the panel of interest for different longitudinal regions along the hull:

for	$x/L>=0.9$	p_s	=	22.52 kN/m^2
for	$x/L<=0.5$	p_s	=	15.12 kN/m^2
for	$0.5<x/L<0.9$	p_s	=	8.504 kN/m^2

The correct design pressure which will be used depend now only on the panel longitudinal position on the hull:

	x/L	=	0.158
Finally:	$\boldsymbol{p_s}$	=	**15.120 kN/m^2**

Using logical functions, provided in MS Excel, allows for this process to become automatic, having the program chose automatically the correct values once the geometrical characteristics of a hull have been defined. This approach is favored because it allows a lot of repetitive work to be avoided but moreover because the automated algorithm allows the structural engineer to rapidly modify the lamination scheme and schedule for each panel to optimize the structure.

5.3.2 Lamination scheme and schedule of example Panel 1

In order to obtain equivalent material properties of a sandwich panel to verify if it can withstand the loading demands the lamination scheme and schedule of the example panel has been determined in the following table.

Table 10. Lamination scheme an schedule of a hull side sandwich panel

PLY	MATERIAL	THK [mm]	MODULUS [N/mm2]	$(EI)_i$ [Nmm2/mm]	$(I)_i$ [mm4/mm]
1	MAT 450	1.13	8050	807089	100.260
2	MAT 450	1.13	8050	625176	77.662
3	0/90 GLASS 1225	0.97	26900	1367421	50.833
4	0/90 GLASS 1225	0.97	26900	1025796	38.134
5	BALSA CORE 150Kg/m^3	12.7	4070	711610	174.843
6	MAT 225	0.65	8050	274932	34.153
7	0/90 GLASS 1225	0.97	26900	1695561	63.032
8	0/90 GLASS 1225	0.97	26900	2127922	79.105

The inertia (I), the flexural rigidity (EI), equivalent tensile elasticity modulus (E_{tot}), distance from the neutral fiber of the multi-layer laminate (V), as well as the theoretical bending strength by bending of skins of the sandwich laminate, are calculated in the same manner as for the single skin panel described in the previous chapter and according to **FPV Part B, Ch 4, Sec 1, [4.3.3-a,b]**

E_{tot} = 9192	MPa	Laminate equivalent tensile elasticity modulus
V = 10.16	mm	Distance of the neutral fiber of the multi-layer
(EI) = 9031392	Nmm^2/mm	Flexural rigidity of the multi-layer laminate
(I) = 646.36	mm^4/mm	Inertia of the multi-layer laminate
K = 17	-	Laminates using polyester/vinyl-ester resin

The theoretical bending strength of a layer used to layup the sandwich panel are acquired from the material manufacturer and are verified experimentally. These values are used here as they are much more favorable than the theoretical bending strength obtained by the Rules formula.

Table 11. Bending strength of the materials used for sandwich panel construction

MATERIAL	σ_{br} [N/mm2]
0/90 GLASS 1225	480
MAT 450	98
MAT 225	98

Verification of the strength requirements of the designed laminate against the defined loads is done in accordance with **HSC C.3.8.4.4 SANDWICH LAMINATES**.

.2 Minimum thicknesses of each skin of sandwich laminate plating

Table 12 Layout and minimum thickness requirement for a sandwich skin laminate skin

Material	number	t_i [mm]	t_{tot} [mm]
MAT 450 (ext)	2	1.13	2.26
0/90 GLASS 1225 (ext)	2	0.97	1.94
BALSA CORE 150Kg/m^3	1	12.7	12.7
MAT 225 (int)	1	0.65	0.65
0/90 GLASS 1225 (int)	2	0.97	1.94
total thickness - exterior skin		**[mm]**	**4.20**
total thickness - interior skin		**[mm]**	**2.59**
minimum skin thickness		**[mm]**	2.25

Condition satisfied!

.4 - .5 Bending stress due to the design pressure

p	=	15.12 kN/m^2	Design pressure
SF	=	6 -	as per table C3.8.5 (HSC)
M	=	293.83 Nmm	Bending moment

Table 13. Hull side plating sandwich skin bending stress

Ply	Material	σ_d		σ_{de}
1	MAT 450	2.69 MPa	<	16.33 MPa
3	0/90 GLASS 1225	9.99 MPa	<	80.00 MPa
6	MAT 225	2.03 MPa	<	16.33 MPa
8	0/90 GLASS 1225	8.50 MPa	<	80.00 MPa

Satisfied!

.6 - .7 Shear stress (core) due to the design pressure

τ_d	=	0.34	MPa	Shear stress in the core due to the design pressure
τ_{de}	=	0.99	MPa	Admissible shear stress in the core
			$\boldsymbol{\tau_d < \tau_{de}}$	**Condition satisfied!**

.8 Bending deflection due to the design pressure

μ_2	=	1.00	-	coefficient defined in C3.8.4.3.8
μ_3	=	1.00	-	coefficient defined in C3.8.4.4.4
f_{be}	=	0.79	mm	Bending deflection (as per C3.8.4.4.8 (HSC))
f_{sh}	=	0.40	mm	Shear deflection (as per C3.8.4.4.8 (HSC))
f	=	1.20	mm	as per 3.8.4.4 - 8 (HSC)
f_{max}	=	6.25	mm	as per 3.8.4.4 - 8 (HSC)
			$\boldsymbol{f < f_{max}}$	**Condition satisfied!**

5.3.3 Side plating report

The same procedure is applied to the other side panels. Lamination scheme and schedule of the sandwich was kept the same throughout the hull side (panels 1 - 11), and the laminate satisfied the load requirements.

5.4 LONGITUDINAL STIFFENERS

Longitudinal stiffeners are omega-type i.e. top-hat type stiffeners made out of polyurethane foam (closed cell) which gives the shape and the dimensions laminated over with hybrid glass-carbon bidirectional reinforcement with high strength unidirectional carbon reinforcement added into the top flange, far from the neutral axis, to give the best overall strength results.

Longitudinal stiffeners are to be infused together with the hull plating.

The division of the longitudinal stiffeners between neighboring transversal stiffeners or bulkheads has been determined for the sake of the calculation and is represented in the following drawing:

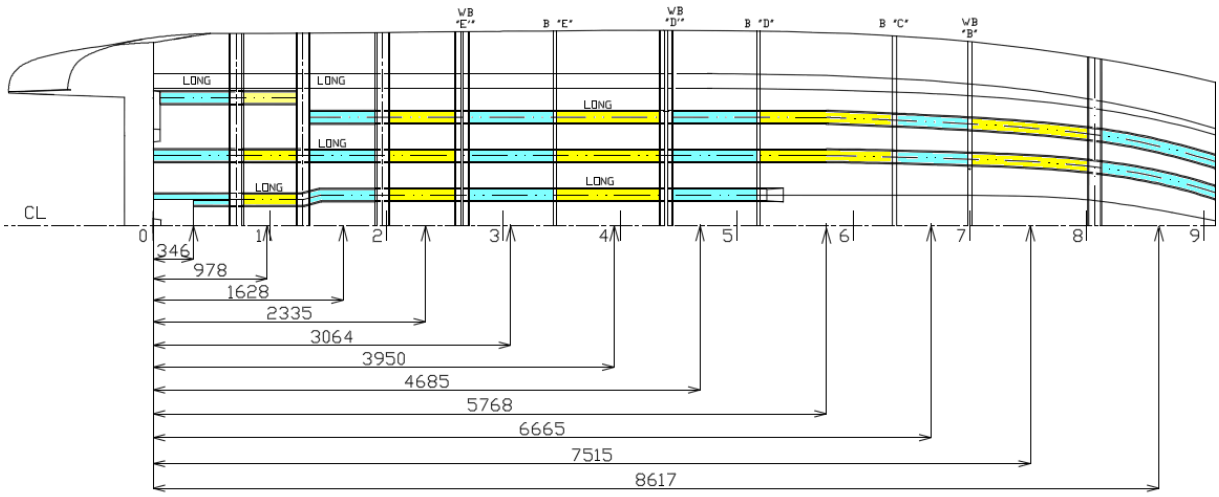

Figure 24. Longitudinal stiffeners division

Table 14. Geometrical characteristics of longitudinal bottom stiffeners

STIFF	long 356	long 998	long 1627	long 2335	long 3064	long 3951	long 4684	long 5768	long 6665	long 7515	long 8617
x[m]	0.356	0.978	1.6275	2.335	3.064	3.95	4.685	5.768	6.665	7.515	8.617
αd [°]	19.150	19.334	19.430	19.820	20.600	21.940	23.890	26.880	30.000	30.000	30.000
s [m]	0.399	0.399	0.353	0.354	0.355	0.359	0.365	0.375	0.365	0.350	0.350
l [m]	0.692	0.452	0.565	0.610	0.668	0.938	0.668	1.131	0.636	1.042	1.042

x[m] - distance from AP to the center of the panel
αd [°] - deadrise angle
s [m] - spacing of stiffeners, measured along the plating
l [m] - overall span of stiffeners

5.4.1 Longitudinal hull bottom stiffener example – long 346"

GEOMETRICAL CHARACTERISTICS

To show the course of the stiffener calculation an example procedure for stiffener "long 346", first from the AP, will be demonstrated.

Table 15. Geometrical characteristics of example hull side sandwich panel 1

dist	0.346	m	Distance from AP
l	0.692	m	Overall span of stiffeners
s	0.399	m	Spacing of stiffeners,measured along the plating
αd	19.150	°	Deadrise angle
a	0.120	m	Stiffeners bottom width
Z	1.065	m	Vertical distance from the moulded base line to load point
f	0	m	Curvature offset of the shell plating

DEFINITIONS AND SYMBOLS **(FPV Part B, Ch 1, Sec 2, [2.1.1])**

Main symbols and definitions defined in FPV, Part B, Ch 1, Sec 2, [2.1.1] and reported in Table 15 for the plating (bottom single skin, and side sandwich) are still valid.

VERTICAL ACCELERATION AT LCG **(FPV Part B, Ch 5, Sec 2, [1.1])**

Also the vertical accelerations and their longitudinal distribution defined in (FPV, Part B, Ch 5, Sec 2, [1.1]) are the same as for the bottom and side plating reported in the previous chapters.

IMPACT PRESSURE ON THE BOTTOM OF HULL **(FPV Part B, Ch 5, Sec 2, [3.3.1])**

The impact pressure due to slamming effects will be considered as the design pressure because it is recognized as the dominant and most dangerous for the longitudinal bottom stiffeners. Impact pressures are calculated in the same way as for the hull bottom plating and the results are the following:

S_r = 10.12 m^2 Reference area

K_1	=	1.00	-	Longitudinal bottom impact pressure distribution factor
S	=	0.80	m^2	Area supported by the element
u	=	7.88	-	
K_2	=	0.50	-	Factor accounting for impact area (>=0.5 for plating) Calculated -> 0.291
α_d	=	19.15	°	deadrise angle
α_{cg}	=	18.00	°	deadrise angle at LCG (10°<αcg<30°)
K_3	=	0.77	-	factor accounting for shape and deadrise of the hull
$\boldsymbol{p_{si}}$	=	**145.72 kN/m²**		Impact pressure acting on the bottom of hull

STIFFENER MAIN DATA

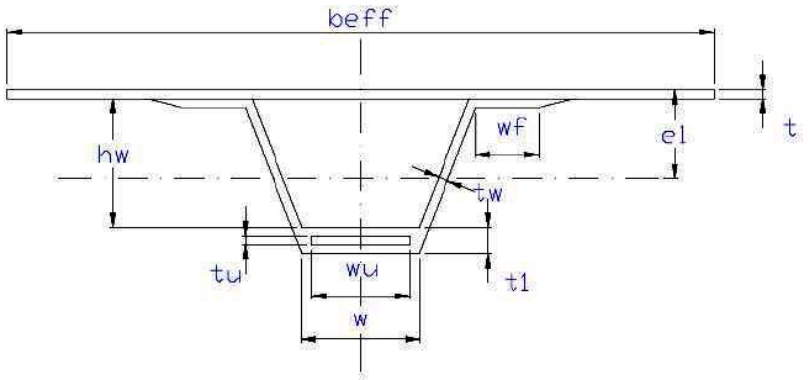

Figure 25. Stiffener main dimensions

hw	=	650	mm
wf	=	50	mm
w	=	100	mm
wu	=	100	mm

FIBRE-REINFORCED PLASTIC CRAFT - HSC

STIFFENERS (*HSC C3.8.4.5*)

l_b	=	328.4	mm	Width of the attached plating
ε	=	1.0	-	Coefficient to take account of the actual conditions of fixation of a stiffener

5.4.2 Stiffeners lamination schedule

Table 16. Stiffener lamination scheme and schedule - Longitudinal bottom stiffener 346

wf	**Material**	**N°**	**ti [mm]**	**t tot [mm]**
	+/- 45 Glass Carbon 820	4	0.90	3.6
tw	**Material**	**N°**	**ti [mm]**	**t tot [mm]**
	+/- 45 Glass Carbon 820	4	0.90	3.6
tl	**Material**	**N°**	**ti [mm]**	**t tot [mm]**
	+/- 45 Glass Carbon 820	2	0.90	1.8
	MAT 225	1	0.65	2.45
	UNITAPE 820 Carbon	3	1	5.45
	+/- 45 Glass Carbon 820	2	0.90	7.25

5.4.3 Associated panel lamination schedule

Table 17 Associated panel lamination schedule - Longitudinal bottom stiffener 346

	Material	**N°**	**t_i [mm]**	**t_{tot} [mm]**
t	MAT 450	2	1.13	2.26
	0/90 GLASS 1225	8	0.97	10.02
	±45 GLASS 1225	3	0.97	12.93

INERTIA CALCULATION (STIFFNER AND ASSOCIATED PANEL)

I	=	5.99E+08	mm^4	Inertia of the stiffener
E	=	2.77E+04	N/mm^2	Equivalent elasticity modulus of a multi-layer stiffener
(EI)	=	1.66E+13	Nmm^2	Flexural rigidity
V	=	259.06	mm	Distance from the stiffener neutral axis to the flange
S_a	=	4680.0	mm^2	Cross area of the stiffener

BENDING MOMENT

p	=	145.718	MPa	Design pressure
M	=	10086216	Nmm	Bending moment acting on the stiffener

BENDING STRESS DUE TO THE DESIGN PRESSURE

Structural fabric considered in the calculation is the top layer of **UNITAPE Carbon 820**, located in the stiffener's hat laminate.

SF	=	4.5	-	Safety factor
σ_d	=	**6.671**	**MPa**	Bending stress
σ_{de}	=	**215.556**	**MPa**	Admissible stress
			$\sigma_d < \sigma_{de}$	**Condition satisfied!**

SHEAR STRESS DUE TO THE DESIGN PRESSURE

SF	=	4.5	-	Safety factor
τ_d	=	**12.41**	**MPa**	Bending stress
τ_{de}	=	**60.00**	**MPa**	Admissible stress
			$\tau_d < \tau_{de}$	**Condition satisfied!**

Other longitudinal bottom stiffeners are designed following the same procedure and are reported in Chapter 6. STRUCTURAL DRAWINGS.

5.5 TRANSVERSAL STIFFENERS

The transversal hull stiffeners are made out from the same combination of materials as the longitudinal stiffeners. The central bottom part is leveled, on the dimension higher than required by the Rules to more easily incorporate the outfitting (equipment and floors).
Transversal stiffener lamination and dimensions are optimized to satisfy the Rules while minimizing weight and cost.

Transversal hull stiffeners are to be made by hand-layup technique after the hull with the longitudinal stiffeners is infused, cured, and the consumables of the process removed.
The scantling procedure of defining the transversal stiffeners is the same already presented for the hull bottom longitudinal stiffeners. An example stiffener is presented.

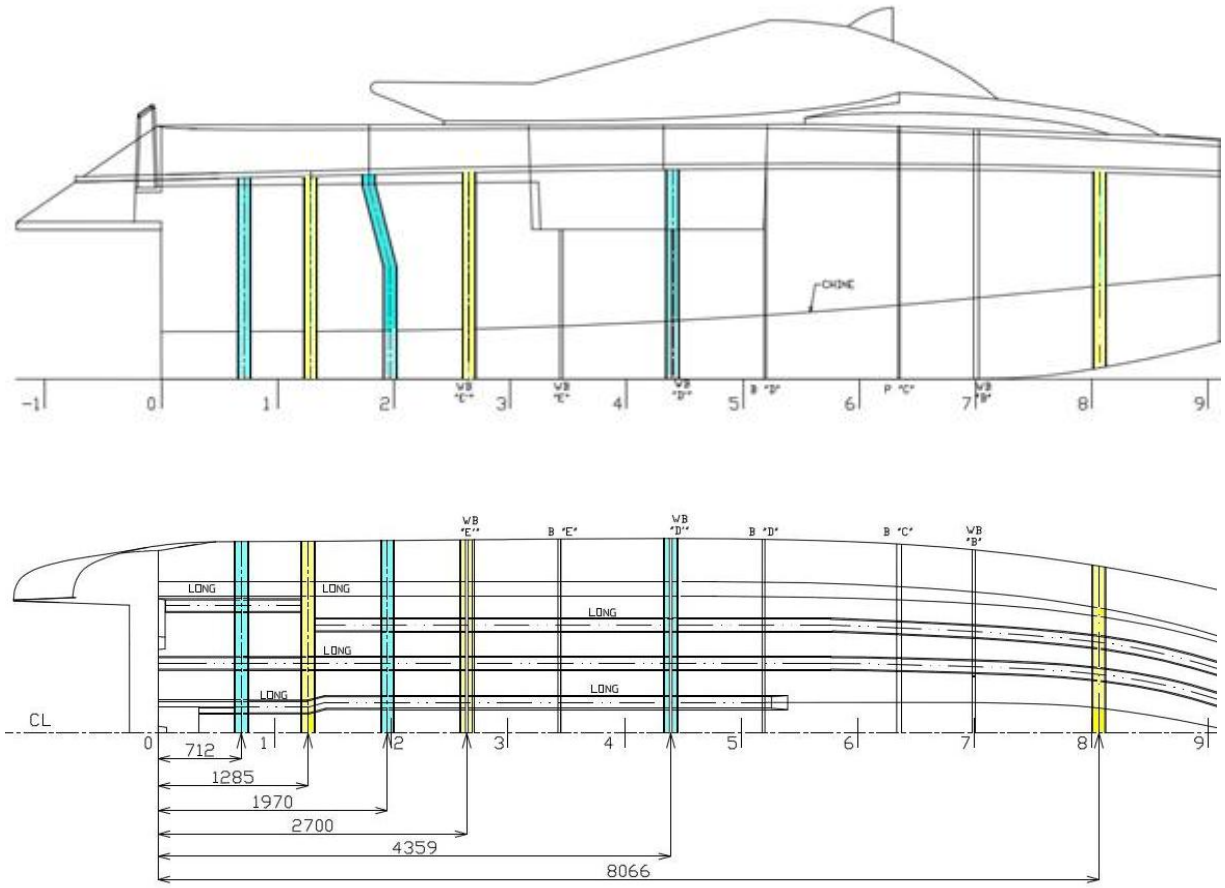

Figure 26. Transversal stiffener division

STIFF	trans 712	trans 1285	trans 1970	trans 2700	trans 4359	trans 8066
x[m]	0.712	1.285	1.97	2.7	4.359	8.066
αd [°]	19.150	19.330	19.580	20.160	22.870	30.000
s [m]	0.642	0.619	0.708	0.729	0.863	1.042
l [m]	1.360	1.362	1.364	1.370	1.401	1.040

x[m] - distance from AP to the center of the panel
αd [°] - deadrise angle
s [m] - spacing of stiffeners, measured along the plating
l [m] - overall span of stiffeners

Figure 27. Geometrical charecteristics of the transversal stiffeneners

5.5.1 Transversal hull bottom stiffener example – trans 1285

GEOMETRICAL CHARACTERISTICS

To show the course of the stiffener calculation an example procedure for stiffener „trans 1285“ will be demonstrated.

Table 18. Geometrical characteristics of example hull side sandwich panel 1

dist	1.2850	m	Distance from AP
l	1.362	m	Overall span of stiffeners
s	0.619	m	Spacing of stiffeners,measured along the plating
αd	19.33	°	Maximum service speed
a	0.120	m	Stiffeners bottom width

DEFINITIONS AND SYMBOLS (**FPV Part B, Ch 1, Sec 2, [2.1.1]**)

Main symbols and definitions defined in FPV, Part B, Ch 1, Sec 2, [2.1.1] and reported in Table 18 for the plating (bottom single skin, and side sandwich) are still valid.

VERTICAL ACCELERATION AT LCG (**FPV Part B, Ch 5, Sec 2, [1.1]**)

Vertical accelerations and their longitudinal distribution defined in (FPV, Part B, Ch 5, Sec 2, [1.1]) are the same as for the bottom plating reported in the previous chapters.

IMPACT PRESSURE ON THE BOTTOM OF HULL (**FPV Part B, Ch 5, Sec 2, [3.3.1]**)

For the design pressure considered being the governing load on the bottom transversal is the impact pressure due to slamming effects. Impact pressures are calculated in the same way as for the hull bottom plating and the results are the following:

S_r	=	10.12	m^2	Reference area
K_1	=	0.62	-	Longitudinal bottom impact pressure distribution factor
S	=	0.84	m^2	Area supported by the element
u	=	8.33	-	
K_2	=	0.50	-	Factor accounting for impact area (>=0.5 for plating) Calculated -> 0.291
α_d	=	19.33	°	deadrise angle
α_{cg}	=	18.00	°	deadrise angle at LCG (10°<αcg<30°)
K_3	=	0.97	-	factor accounting for shape and deadrise of the hull
$\boldsymbol{p_{si}}$	=	**115.35 kN/m²**		Impact pressure acting on the bottom of hull

STIFFENER MAIN DATA

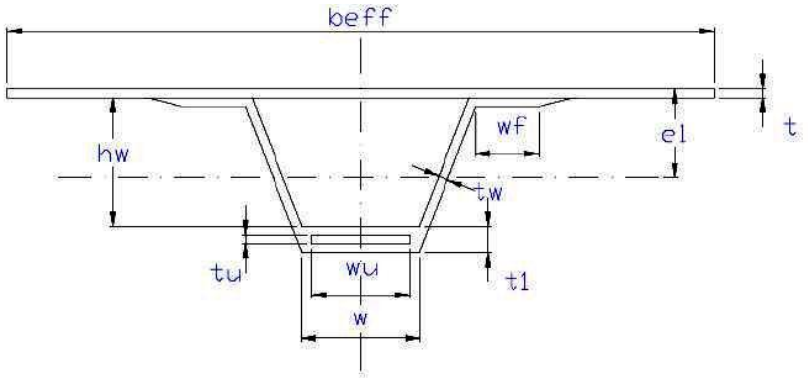

Figure 28. Stiffener main dimensions

hw	=	100	mm
wf	=	50	mm
w	=	100	mm
wu	=	100	mm

FIBRE-REINFORCED PLASTIC CRAFT - HSC

STIFFENERS (*HSC C3.8.4.5*)

l_b	=	394.4	mm	Width of the attached plating
ε	=	1.0	-	Coefficient to take account of the actual conditions of fixation of a stiffener

5.5.2 Stiffeners lamination schedule

Table 19. Stiffener lamination scheme and schedule - Longitudinal bottom stiffener 346

	Material	N°	ti [mm]	t tot [mm]
wf	+/- 45 Glass Carbon 820	5	0.9	4.5
	Material	**N°**	**ti [mm]**	**t tot [mm]**
tw	+/- 45 Glass Carbon 820	5	0.9	4.5
	Material	**N°**	**ti [mm]**	**t tot [mm]**
tl	+/- 45 Glass Carbon 820	2	0.9	1.8
	MAT 225	1	1	2.8
	UNITAPE 820 Carbon	4	0.65	5.4
	+/- 45 Glass Carbon 820	3	0.9	8.1

5.5.3 Associated panel lamination schedule

Table 20. Associated panel lamination schedule - Longitudinal bottom stiffener 346

	Material	N°	t_i [mm]	t_{tot} [mm]
t	MAT 450	2	1.13	2.26
	0/90 GLASS 1225	7	0.97	9.05

INERTIA CALCULATION (STIFFNER AND ASSOCIATED PANEL)

I	=	1.09E+07	mm^4	Inertia of the stiffener
E	=	3.16E+04	N/mm^2	Equivalent elasticity modulus of a multi-layer stiffener
(EI)	=	3.46E+11	Nmm^2	Flexural rigidity
V	=	30.45	mm	Distance from the stiffener neutral axis to the flange
S_a	=	900.0	mm^2	Cross area of the stiffener

BENDING MOMENT

p	=	115.35	MPa	Design pressure
M	=	11037513	Nmm	Bending moment acting on the stiffener

BENDING STRESS DUE TO THE DESIGN PRESSURE

Structural fabric considered in the calculation is the top layer of **UNITAPE Carbon 820**, located in the stiffener's hat laminate.

SF	=	4.5	-	Safety factor
σ_d	=	**74.14**	**MPa**	Bending stress
σ_{de}	=	**304.44**	**MPa**	Admissible stress

$\sigma_d < \sigma_{de}$ **Condition satisfied**!

SHEAR STRESS DUE TO THE DESIGN PRESSURE

SF	=	3.5	-	Safety factor
τ_d	=	**54.03**	**MPa**	Bending stress
τ_{de}	=	**65.71**	**MPa**	Admissible stress

$\tau_d < \tau_{de}$ **Condition satisfied!**

The same procedure is applied for the other transversal stiffeners and the result is presented in Chapter 6. STRUCTURAL DRAWINGS.

6 STRUCTURAL DRAWINGS

7 Lamination scheme and schedule

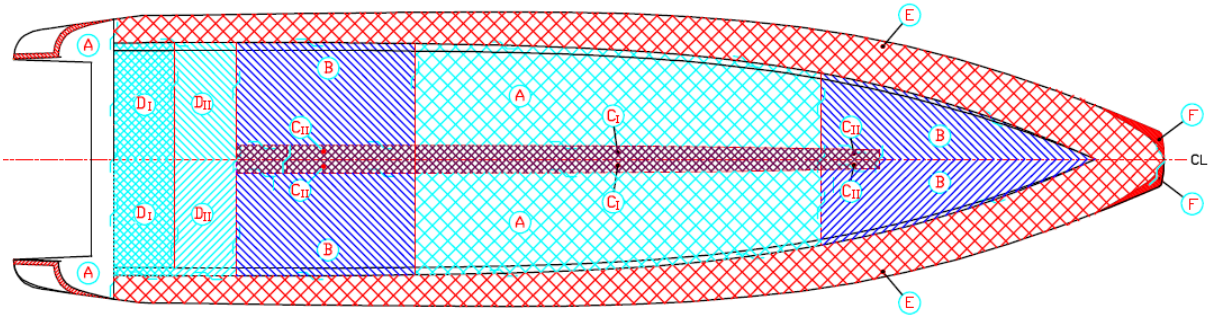

Figure 29. Plan view of hull lamination plan

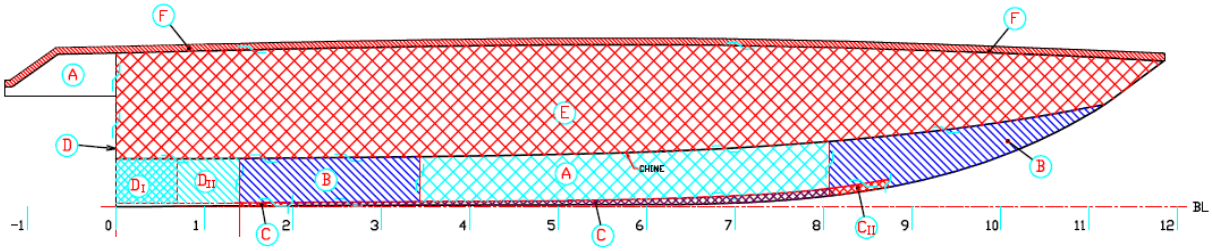

Figure 30. Hull lamianation plan – Lateral view

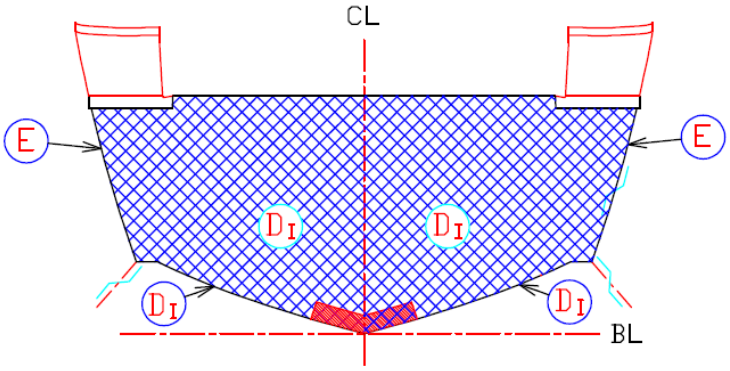

Figure 31.Transom lamination plan

Table 21. Lamination scheldule of the hull

LAMINATION SCHEDULE										
TYPE OF REINFORCEMENT		UNIT THICKENSS mm	TOTAL THICKENESS							
			A	B	C_I	C_{II}	D_I	D_{II}	E	F
0	GELCOAT (600 gr/mq)	-	X	X	X	X	X	X	X	
1	MAT 450	1.13	1.13	1.13	1.13	1.13	1.13	1.13	1.13	1.13
2	MAT 450	1.13	2.26	2.26	2.26	2.26	2.26	2.26	2.26	2.26
2a	0°/90° GLASS E 1225	1.16					3.42	3.42		
2b	0°/90° GLASS E 1225	1.16					4.58			
3	0°/90° GLASS E 1225	0.97	3.23	3.23	3.23	3.23	5.55	4.39	3.23	3.23
4	0°/90° GLASS E 1225	0.97	4,2	4,2	4,2	4,2	6,52	5.36	4,2	4,2
5	0°/90° GLASS E 1225	0.97	5.17	5.17	5.17	5.17	7.49	6.33		
6	0°/90° GLASS E 1225	0.97	6.14	6.14	6.14	6.14				5.17
7	BALSA CORE 150Kg/m^3	12.7							16.9	
8	MAT 450	0.94							17.84	
9	+-45° GLASS E 1225	0.97					8.46	7.3		
10	+-45° GLASS E 1225	0.97					9,43	8,27		
11	+-45° GLASS E 1225	0.97					10,4	9,24		
12	0°/90° GLASS E 1225	0.97	7.11	7.11	7.11	10.06	11.37	10.21		
13	0°/90° GLASS E 1225	0.97	8.08	8.08	8.08	8.08	12.34	11.18	18.81	6.14
14	0°/90° GLASS E 1225	0.97	9.05	9.05	9.05	9.05	13.31	12.15	19.78	7.11
15	0°/90° GLASS E 1225	0.97	10.02		10.02					

7.1 Hull structure

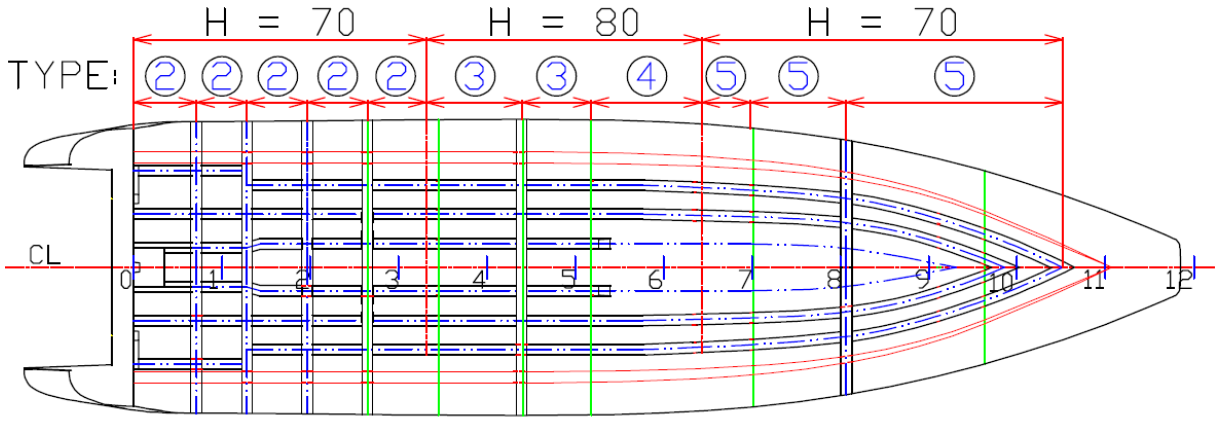

Figure 32.Bottom stiffeners

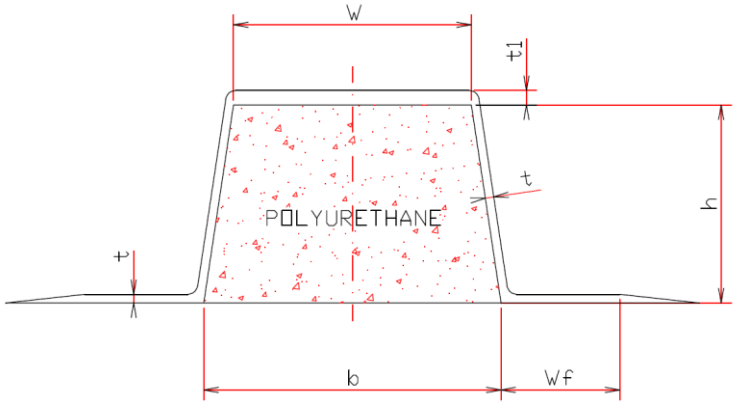

Figure 33. Stiffener dimension

Table 22. Reinforcement dimensions

	REINFORCEMENT TYPE												
	1	2	3	4	5	6	7	8	9	10	11	12	13
h	70	70	80	80	70	100	120	155	155	70	85	120	70
b	120	120	120	120	120	120	120	120	120	120	120	120	120
W	100	100	100	100	100	100	100	100	100	100	100	100	100
Wf	50	50	50	50	50	50	50	50	50	50	50	50	50
t	3,5	2,5	2,5	4,5	3,5	4,5	4,5	5,5	4,5	2,5	2,5	5,5	5,5
t_1	3,5	4,5	5,5	8	7,5	9,0	9,0	11	8,0	5,5	5,5	10	10

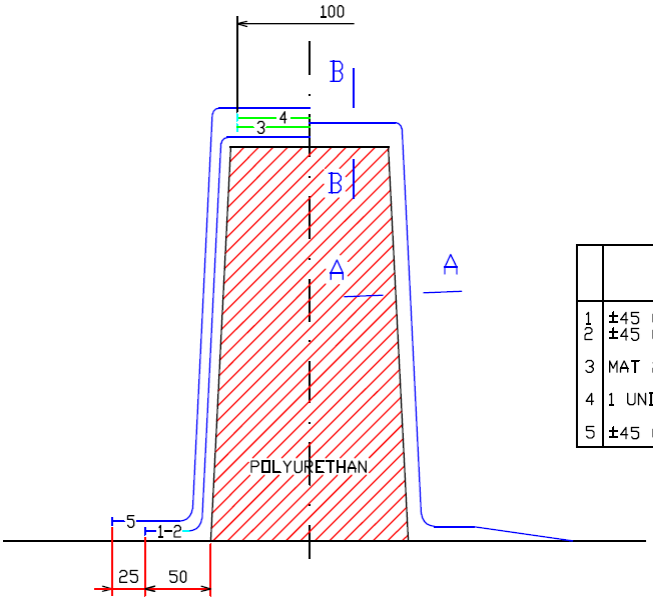

	REINFORCEMENT TYPE	RATIO R/V	UNIT THICK. mm	TOTALE THICKNESS A	TOTALE THICKNESS B
1	±45 GLASS/CARBON 820	0,85:1	0,90	0,90	0,90
2	±45 GLASS/CARBON 820	0,85:1	0,90	1,80	1,80
3	MAT 225	2,4:1	0,65		2,45
4	1 UNITAPE CARBON 800	0,85:1	1x1		3,45
5	±45 GLASS/CARBON 820	0,85:1	0,90	2,70	4,35

Figure 34. Typical reinforcement lamination scheme – TYPE 2 reinforcement

Table 23. TYPE 3 reinforcement lamination

	TYPE 3	RATIO R/V	UNIT THICK. mm	TOTALE THICK., mm A	TOTALE THICK., mm B
1	±45 GLASS/CARBON 820	0,85:1	0,90	0,90	0,90
2	±45 GLASS/CARBON 820	0,85:1	0,90	1,80	1,80
3	MAT 225	2,4:1	0,65		2,45
4	2 UNITAPE CARBON 800	0,85:1	1x2		4,45
5	±45 GLASS/CARBON 820	0,85:1	0,90	2,70	5,35

Table 24. TYPE 4 reinforcement lamination

	TYPE 4	RAPPORTO R/V	SPESS. UNIT. mm	SPESSORE TOTALE mm A	SPESSORE TOTALE mm B
1	±45 GLASS/CARBON 820	0,85:1	0,90	0,90	0,90
2	±45 GLASS/CARBON 820	0,85:1	0,90	1,80	1,80
3	±45 GLASS/CARBON 820	0,85:1	0,90	2,70	2,70
4	MAT 225	2,4:1	0,65		3,35
5	3 UNITAPE CARBONIO 800	0,85:1	1x3		6,35
6	±45 GLASS/CARBON 820	0,85:1	0,90	3,60	7,25
7	±45 GLASS/CARBON 820	0,85:1	0,90	4,50	8,15

Table 25. TYPE 5 reinforcement lamination

	TYPE 5	RAPPORTO R/V	SPESS. UNIT. mm	SPESSORE TOTALE mm	
				A	B
1	±45 GLASS/CARBON 820	0,85:1	0,90	0,90	0,90
2	±45 GLASS/CARBON 820	0,85:1	0,90	1,80	1,80
3	MAT 225	2,4:1	0,65		2,45
4	3 UNITAPE CARBONIO 800	0,85:1	1x3		5,45
5	±45 GLASS/CARBON 820	0,85:1	0,90	2,70	6,35
6	±45 GLASS/CARBON 820	0,85:1	0,90	3,60	7,25
7	±45 GLASS/CARBON 820	0,85:1	0,90	4,50	8,15

Table 26. TYPE 6 abd 7 reinforcement lamination

	TYPE 6 and 7	RAPPORTO R/V	SPESS. UNIT. mm	SPESSORE TOTALE mm	
				A	B
1	±45 GLASS/CARBON 820	0,85:1	0,90	0,90	0,90
2	±45 GLASS/CARBON 820	0,85:1	0,90	1,80	1,80
3	MAT 225	2,4:1	0,65		2,45
4	4 UNITAPE CARBONIO 800	0,85:1	1x4		6,45
5	±45 GLASS/CARBON 820	0,85:1	0,90	2,70	7,35
6	±45 GLASS/CARBON 820	0,85:1	0,90	3,60	8,25
7	±45 GLASS/CARBON 820	0,85:1	0,90	4,50	9,15

Table 27. TYPE 8 reinforcement lamination

	TYPE 8	RAPPORTO R/V	SPESS. UNIT. mm	SPESSORE TOTALE mm	
				A	B
1	±45 GLASS/CARBON 820	0,85:1	0,90	0,90	0,90
2	±45 GLASS/CARBON 820	0,85:1	0,90	1,80	1,80
3	MAT 225	2,4:1	0,65		2,45
4	3 UNITAPE CARBONIO 800	0,85:1	1x3		5,45
5	±45 GLASS/CARBON 820	0,85:1	0,90	2,70	6,35
6	±45 GLASS/CARBON 820	0,85:1	0,90	3,60	7,25

Table 28. TYPE 9 reinforcement lamination

	TYPE 9	RAPPORTO R/V	SPESS. UNIT. mm	SPESSORE TOTALE mm	
				A	B
1	±45 GLASS/CARBON 820	0,85:1	0,90	0,90	0,90
2	±45 GLASS/CARBON 820	0,85:1	0,90	1,80	1,80
3	±45 GLASS/CARBON 820	0,85:1	0,90	2,70	2,70
4	MAT 225	2,4:1	0,65		3,35
5	5 UNITAPE CARBONIO 800	0,85:1	1x5		8,35
6	±45 GLASS/CARBON 820	0,85:1	0,90	3,60	9,25
7	±45 GLASS/CARBON 820	0,85:1	0,90	4,50	10,15
8	±45 GLASS/CARBON 820	0,85:1	0,90	5,40	11,05

Table 29. TYPE 12 and 13 reinforcement lamination

	TYPE 12 and 13	RAPPORTO R/V	SPESS. UNIT. mm	SPESSORE TOTALE mm	
				A	B
1	±45 GLASS/CARBON 820	0,85:1	0,90	0,90	0,90
2	±45 GLASS/CARBON 820	0,85:1	0,90	1,80	1,80
3	±45 GLASS/CARBON 820	0,85:1	0,90	2,70	2,70
4	MAT 225	2,4:1	0,65		3,35
5	4 UNITAPE CARBON 800	0,85:1	1x4		7,35
6	±45 GLASS/CARBON 820	0,85:1	0,90	3,60	8,25
7	±45 GLASS/CARBON 820	0,85:1	0,90	4,50	9,15
8	±45 GLASS/CARBON 820	0,85:1	0,90	5,40	10,05

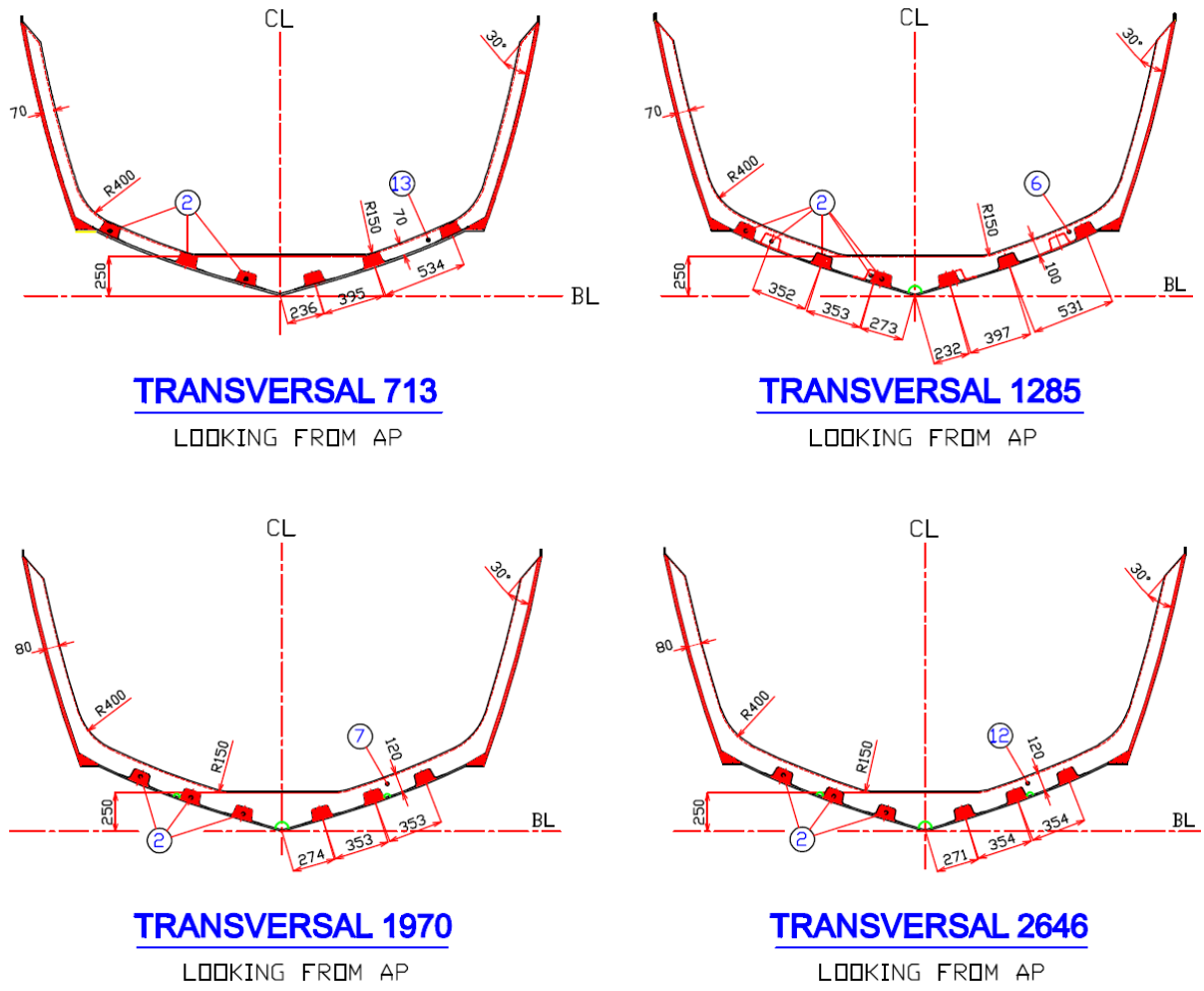

Figure 35. Transversal stiffeners 713 - 2626

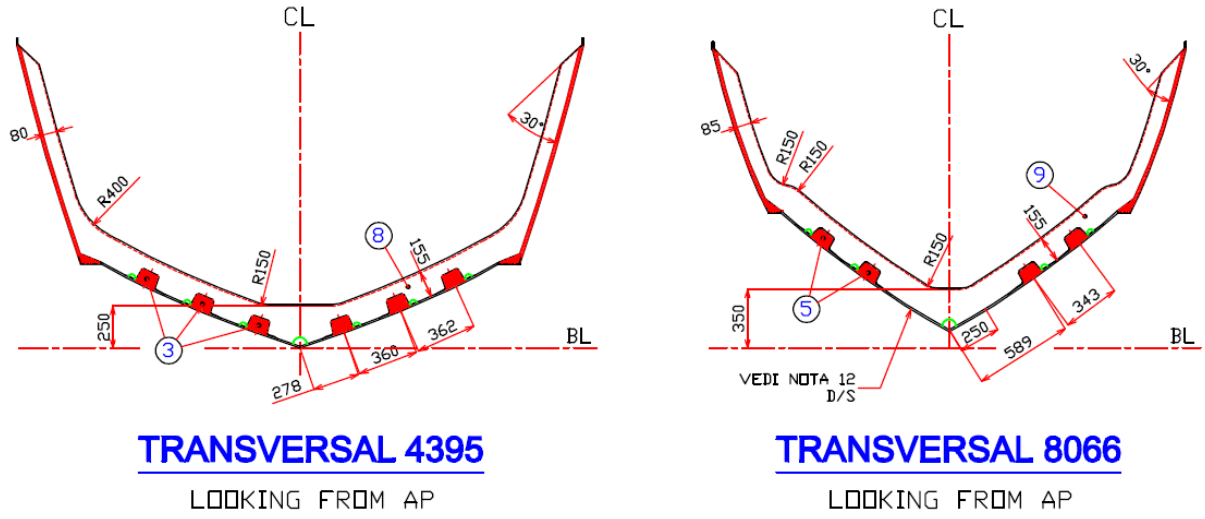

Figure 36. Transversal stiffeners 4395 - 8066

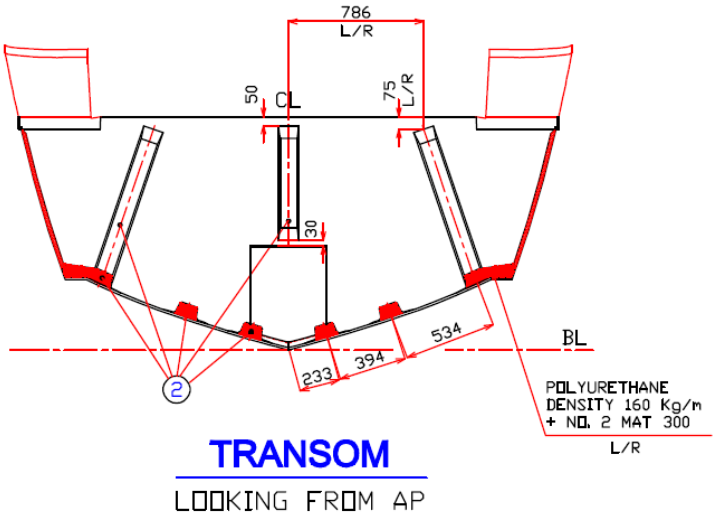

Figure 37. Transom structure drawing

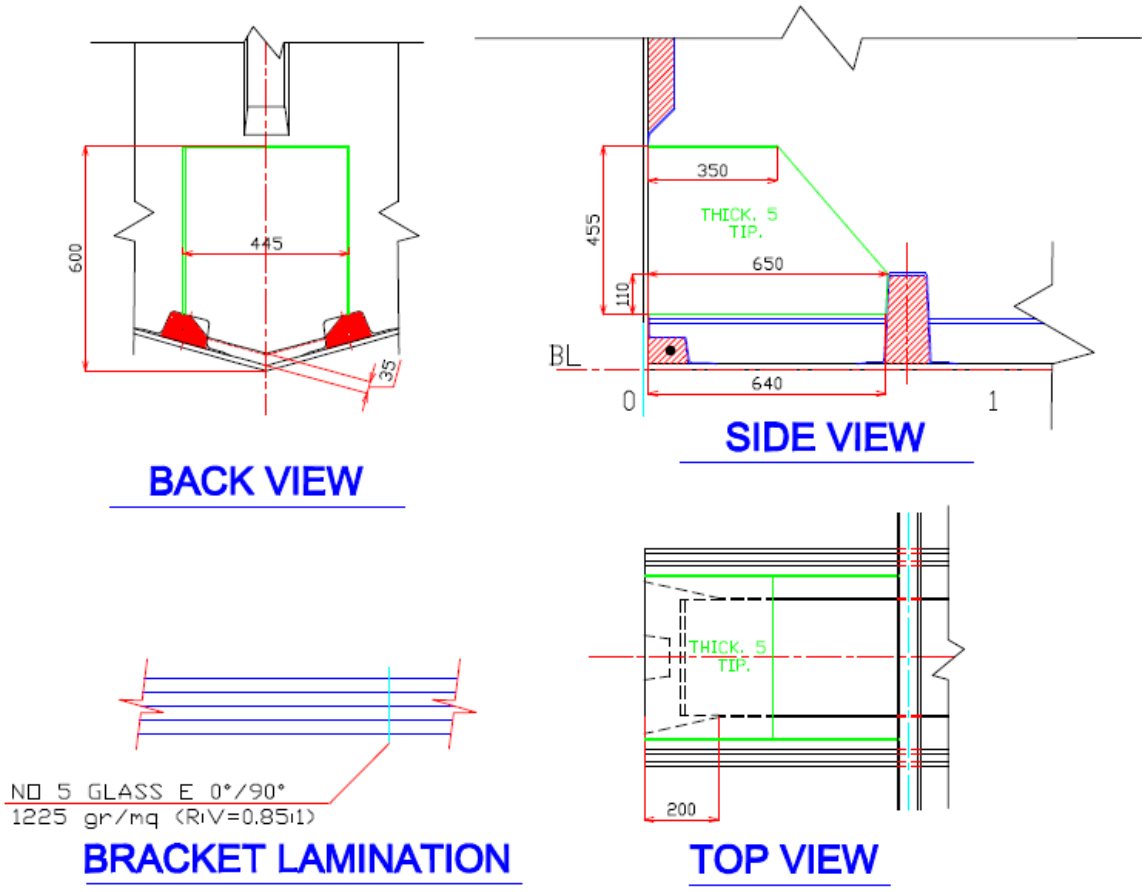

Figure 38.Transom reinforcement bracket

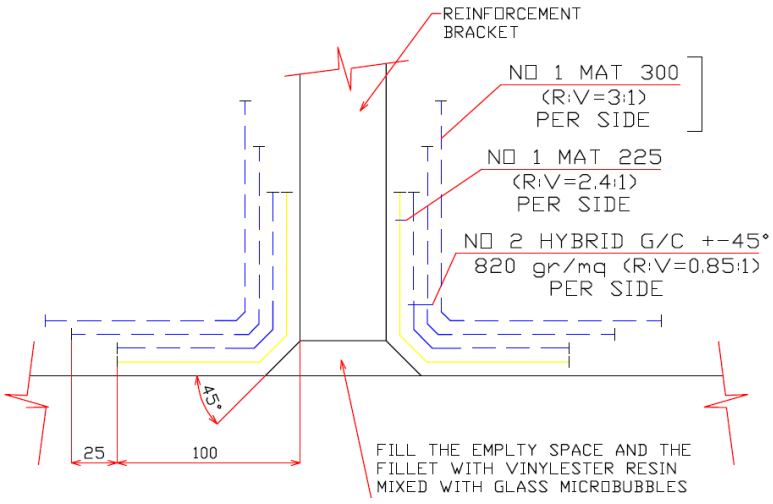

Figure 39.Transom reinforcement bracket connection detail

8 FINITE ELEMENT ANALYSIS OF THE TRANSOM

8.1 Introduction

Finite Element Method (FEM) is a numerical method widely used for structural calculations. As opposite of introducing the method itself this chapter was rather oriented towards noting the possible source of errors for result obtained with this method. As with time commercial FEM software becomes more and more user friendly the most important value of the engineer is not to obtain the result, but to interpret it critically.

To be able to assess the result critically one has to be aware of the following:

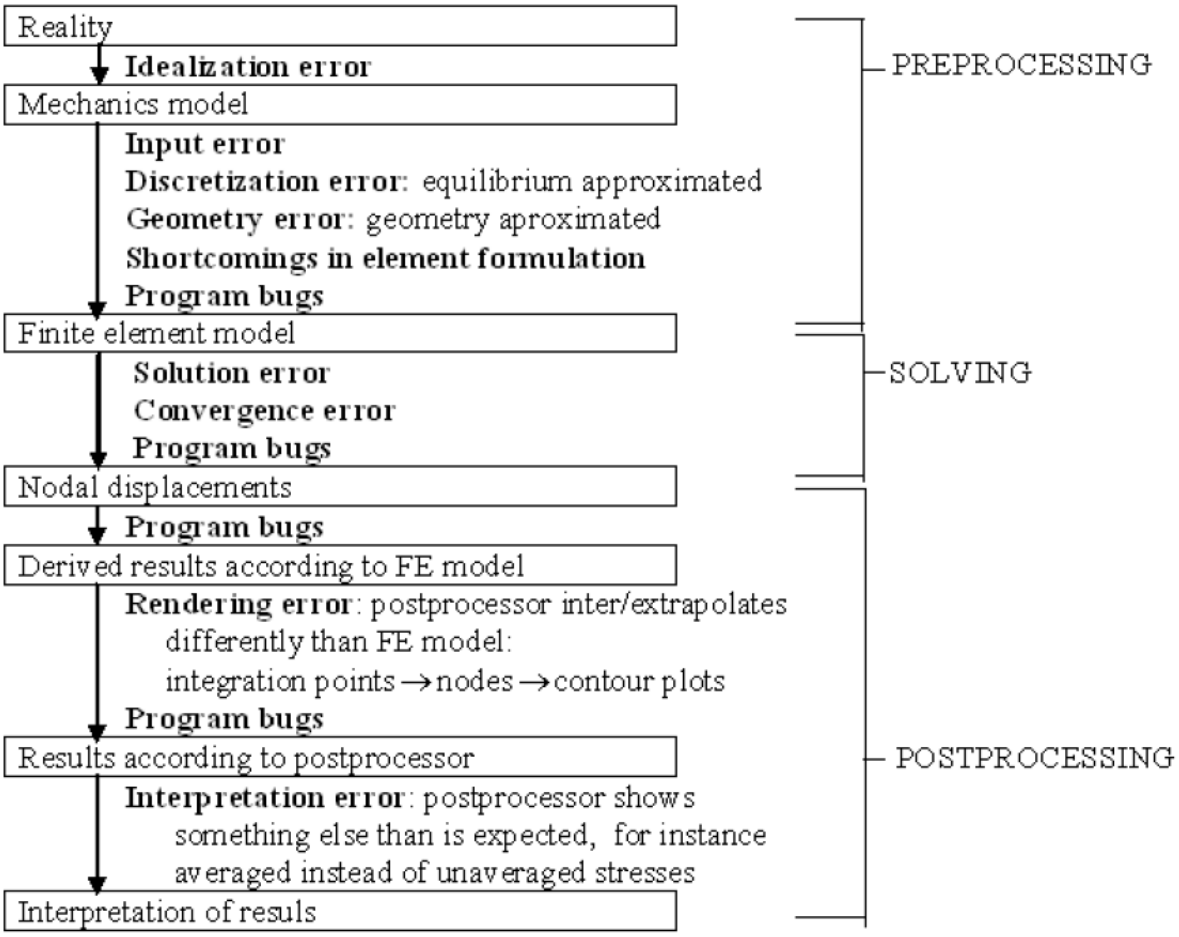

Figure 40. Overview of FEM possbile errors [5]

For the specific project the commercial FEM software ANSYS was used to perform a detail calculation of the transom part of the high speed yacht.
Generally, it is stated by the RINA Code that the structure of the transom should be at least equal or stronger than the aft part of the bottom or the side, whichever is stronger. Thus, the same single skin plating lamination as for the bottom aft plating is kept for the transom, as well as the longitudinal bottom stiffeners are prolonged vertically up the transom as much as the predicted equipment installation allowed. A "bracket" structure is foreseen to distribute the loads in a continuous manner from the transom to the hull bottom structure.But, unlike the reference waterjet project configuration where the thrust loads where accepted by the hull structure via the waterjet bulkhead and the surrounding stiffeners the thrust bearing in the Arnesson SPP (surface piercing propellers) configuration are taken by the transom itself. Such high loads exerted on the transom required a detail calculation to be applied on the transom part.
The FEM simulation to be performed is linear and static but its complexity arises from the fact that the hull is made of composite material which behavior is highly orthotropic and depends on the interaction between the inner layers of the laminate, as for the plating as well as for the stiffeners.

When modeling composites the following steps need to be approach with attention:

- Selection of the proper element type
- Defining the layered configuration
- Specifying Failure criteria

Also it should be noted that composites exhibit several types of coupling effects, such as coupling between bending and twisting, coupling between extension and bending, etc. This is due to stacking of layers of differing material properties. As a result, if the layer stacking sequence is not symmetric, you may not be able to use model symmetry even if the geometry and loading are symmetric, because the displacements and stresses may not be symmetric.

8.2 Model

Building a finite element model begins with a computer-aided design surface model. Surface models are preferable to solid models, although the former can be extracted from the solid model with some additional effort [4].

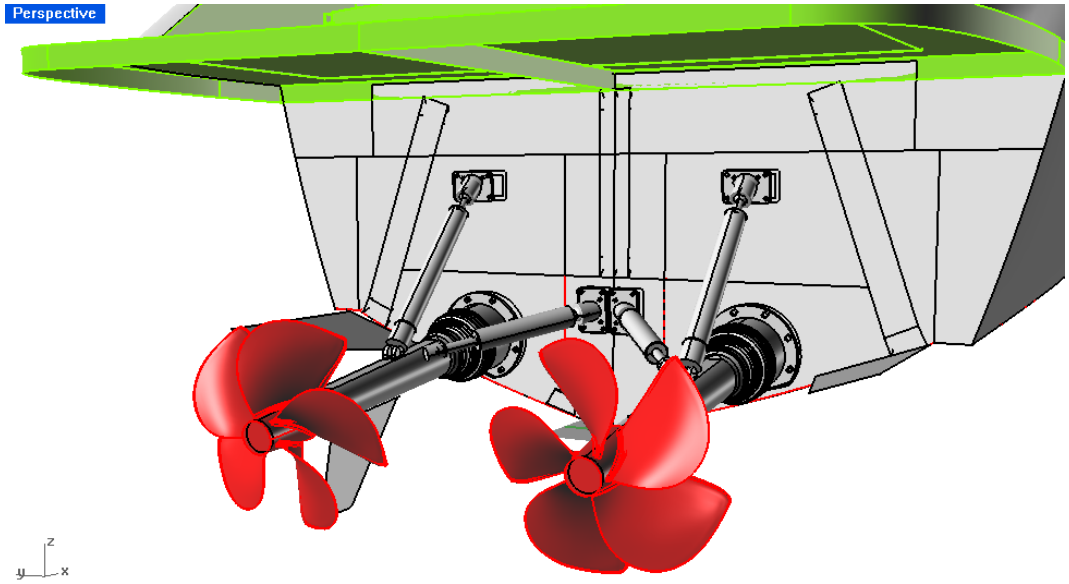

Figure 41. Arrnesson surface drive and transom model

It is possible, in the previous figure, to identify the loading points from the Arnesson SPP drive on the transom structure where the axes connections and the hydraulic cylinders connections are.

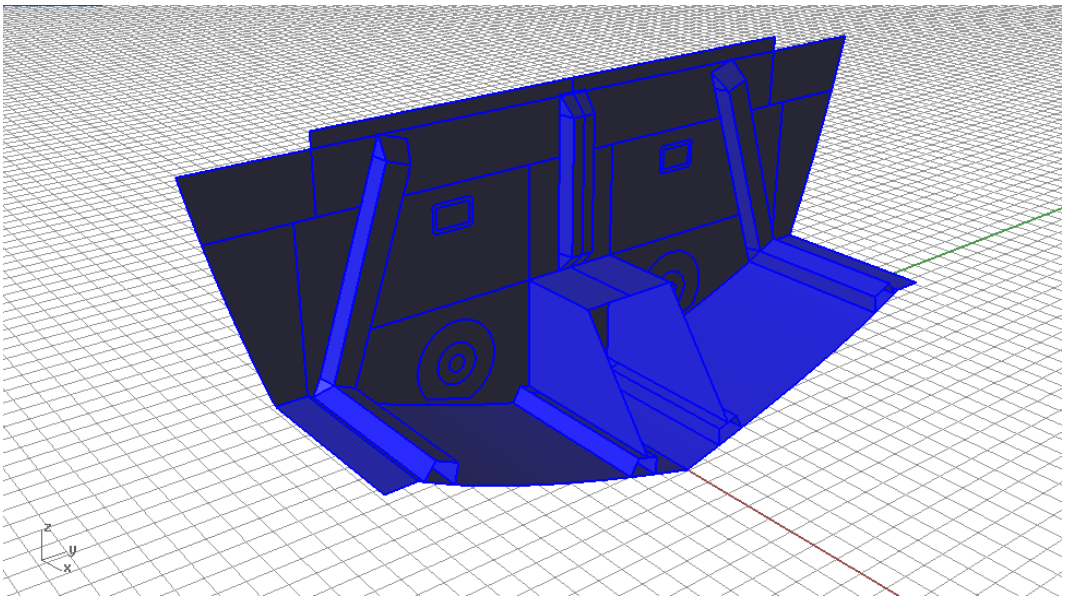

Figure 42. Transom model

The transom structure model to be exported for a FEM simulation was carefully divided in regions (on area per regions), each region defined by a different lamination.

After the model was exported to the ANSYS software it needed to be rechecked for errors. This errors usually arrive from the different logic used for defining curves and areas by NURBS surface modeling programs and simulation software (e.g. FEM or CFD tools).

8.3 SECTION DEFINITION

As stated earlier, every part of the transom structure that has a different lamination scheme has been defined as a different section, shown by a different color in the figure below.

To capture the orthotropic nature of the materials, the properties of different layers, sections are then defined by shell lay-up information.

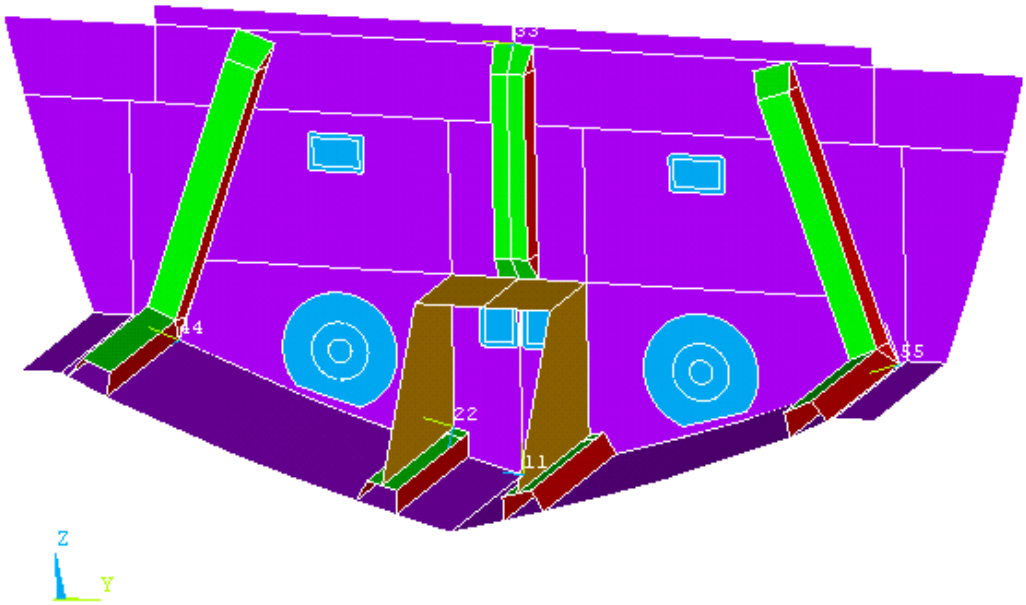

Figure 43. Transom model verified after import and divided in sections

Before proceeding to shell lay-up it is necessary to define the material models used in the simulation. Usually, unlike standard metal construction materials, composite material models are not available in the databases due to a huge variety of possibilities. Thus, it is necessary to rely on manufacturer's datasheets and testing (in-house or not) results.

The following table shows the materials, and their propertied, used for the transom strucuture:

Table 30. Material ID and properties used for section definition in FEM calculation

MATERIAL	STEEL	G/C HYBRID	UNITAPE CARBON	0/90 GLASS	+/-45 GLASS
MAT ID	1	4	5	7	12
EX	2.10E+11	2.65E+10	1.02E+11	1.33E+10	1.73E+10
EY	isotropic	2.65E+10	3.00E+09	1.40E+10	1.69E+10
EZ	isotropic	2.65E+10	3.00E+09	4.20E+09	4.20E+09
NUXY	0.32	0.2	5.88E-03	0.21038	0.19572
NUYZ	isotropic	0.2	0.2	6.00E-02	4.96E-02
NUXZ	isotropic	0.2	5.88E-03	6.32E-02	4.86E-02
GXY	-	2.10E+09	2.10E+09	4.03E+09	4.49E+09
GYZ	-	2.10E+09	2.10E+09	1.75E+09	1.75E+09
GXZ	-	2.10E+09	2.10E+09	1.75E+09	1.75E+09
DENS	7850	1000	1000	1555	1650
PRXY	0.32	0.2	0.2	0.2	0.2
PRYZ	isotropic	0.2	0.2	0.2	0.2
PRXZ	isotropic	0.2	0.2	0.2	0.2

Where in the previous table the listed quantities are:

(EX, EY, EZ) – Elastic moduli [MPa],

(NUXY, NUYZ, NUXZ) – Minor Poission's ratio

(GXY, GYZ, GXZ) – Shear moduli [MPa]

(DENS) – Density [kg/m^3]

(PRXY, PRYZ, PRXZ) – Major Poisson's ratio

Once the material model database has been created it is possible to define the shell lay-up. It is recommended to use "false layers" to level the same material in different sections to facilitate the post-processing and the interpretation of the results later. This is due to the fact that the post-processing is done layer-by-layer.

Using "false layers" means defining layer of random material with zero thickness to push up or down other layers in the section to level them with the same or similar material layer.

False layer e.g.: The steel plates of the propulsion drive connecting to the composite structure of the transom are included in the model. To avoid the steel plate layer being leveled with the same layer, for post-processing, with one of the reinforcement layers a false first layer was defined on all sections except the ones representing the connections. This can be seen in the table showing the shell lay-up below:

Table 31. Shell lay-up connecting material ID with section ID's

SECTION		MATERIAL ID LAYOUT			
Name	ID	Layer 1	Layer 2	Layer 3	Layer 4
Transom	2	-	7	12	7
Stiffener side	3	-	4	-	-
Connections	4	1	7	12	7
Stiffener head	6	-	4	5	4
Bracket	7	-	7	-	-

It is important to note, while interpreting the previous table, that the layers in a section are dependent on when the material changes, i.e., several layers of the same material are defined as one layer with the corresponding thickness.

Having defined the material database ID's and the shell-lay-up the multi-layered, orthotropic structure of the model has been defined. This process needs to be done with great care. It is also necessary to keep in mind how the local mesh element coordinate system will be orientated, as will be discussed later, to adjust the ply orientation in the shell definition accordingly.

For an example, if considering the unidirectional carbon reinforcement in the head of the stiffeners, it has very high load-carrying capacities in the direction of the fiber but poor perpendicular to them. If the ply orientation is set to 0° it means that the fibers are orientated in the x-direction of each element (which is discretizing the stiffeners heads) local coordinate system by default. This furthermore implies that the orientation of element local coordinate systems of each section needs to be chosen with care.

8.4 Meshing

ANSYS has an integrated mesher which allows easy meshing with good control. One of the key factors to obtain realistic results is to choose an appropriate mesh element type for the type of the simulation. There is a comprehensive guide with a theory reference available in ANSYS to help the user choose the appropriate one.

Section definition and detail mesh control are not possible using ANSYS Workbench which is a user-friendly interface to use the ANSYS modules. Thus, it is not possible to model composites using the Workbench but rather using ANSYS Mechanical APDL module which also allows more in-depth control of the parameter but lacks the user-friendliness making simulations more tedious and long-lasting except for professional users.
For a standard composite simulation mesh element type SHELL181 is recommended.

8.4.1 ELEMENT TYPE: SHELL181 4-Node Structural Shell

SHELL181 [6] is suitable for analyzing thin to moderately-thick shell structures. It is a four-node element with six degrees of freedom at each node: translations in the x, y, and z directions, and rotations about the x, y, and z-axes. (If the membrane option is used, the element has translational degrees of freedom only). The degenerate triangular option should only be used as filler elements in mesh generation.
SHELL181 is well-suited for linear, large rotation, and/or large strain nonlinear applications. Change in shell thickness is accounted for in nonlinear analyses. In the element domain, both full and reduced integration schemes are supported. SHELL181 accounts for follower (load stiffness) effects of distributed pressures.
SHELL181 may be used for layered applications for modeling composite shells or sandwich construction. The accuracy in modeling composite shells is governed by the first-order shear-deformation theory (usually referred to as Mindlin-Reissner shell theory).
The element formulation is based on logarithmic strain and true stress measures. The element kinematics allow for finite membrane strains (stretching). However, the curvature changes within a time increment are assumed to be small.
The following figure shows the geometry, node locations, and the element coordinate system for this element. The element is defined by shell section information and by four nodes (I, J, K, and L).

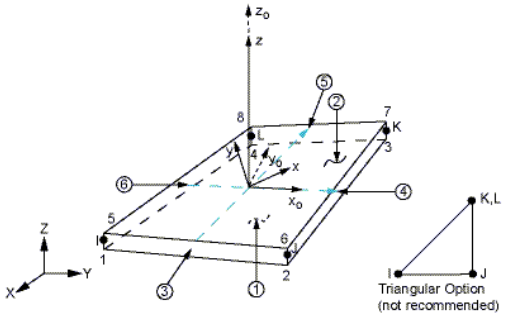

Figure 44. Shell element geometry

8.4.2 Mesh presentation

Having chosen the relevant mesh parameters mentioned before a mesh model of the transom part has been generated.

.

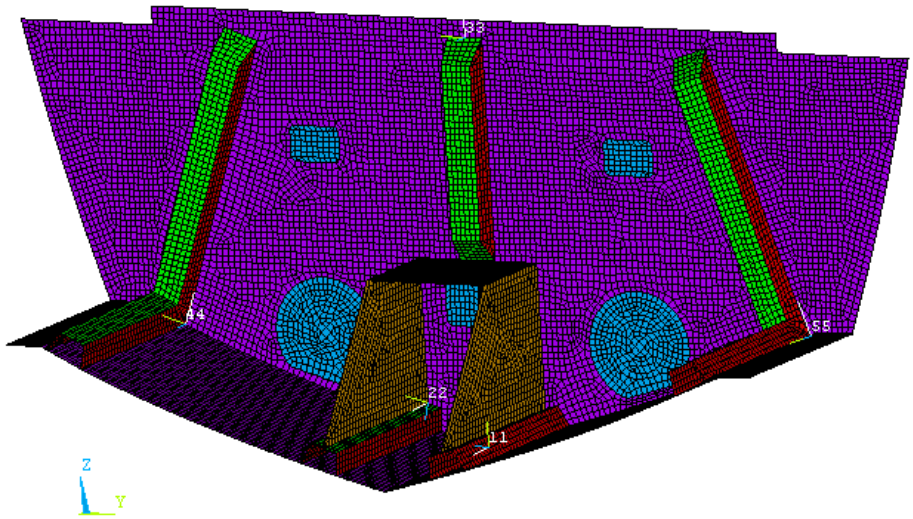

Figure 45. Transom mesh

The part was meshed with 19282 elements. Base size of the quadratic element used is 0.02 meters. Triangular elements and smaller size elements were used only where necessary to produce a good quality mesh.

The following figure shows a meshed part detail with the visual representation of the shell lay-up showing different layers and their thicknesses now defined as a mesh property.

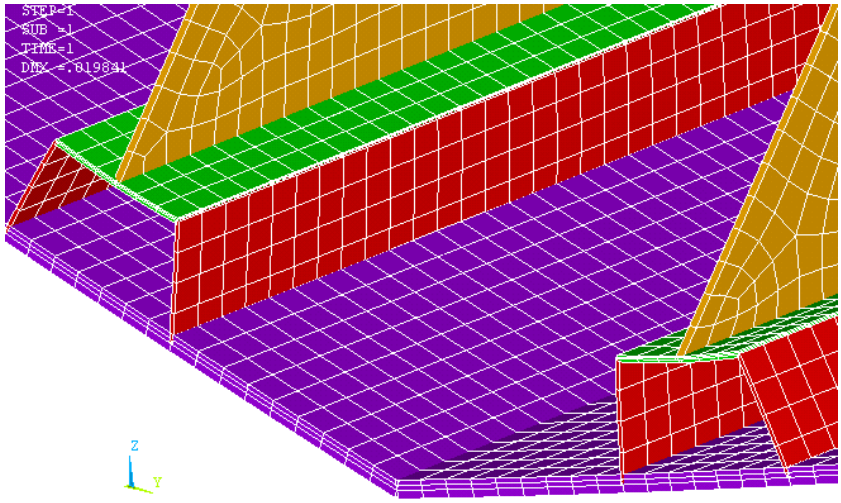

Figure 46. Section shape turned on for different layer perception

The following figures show an example of the elements' local coordinate system orientations. As stated earlier they are very important to properly orientate the orthotropic properties of different plies.

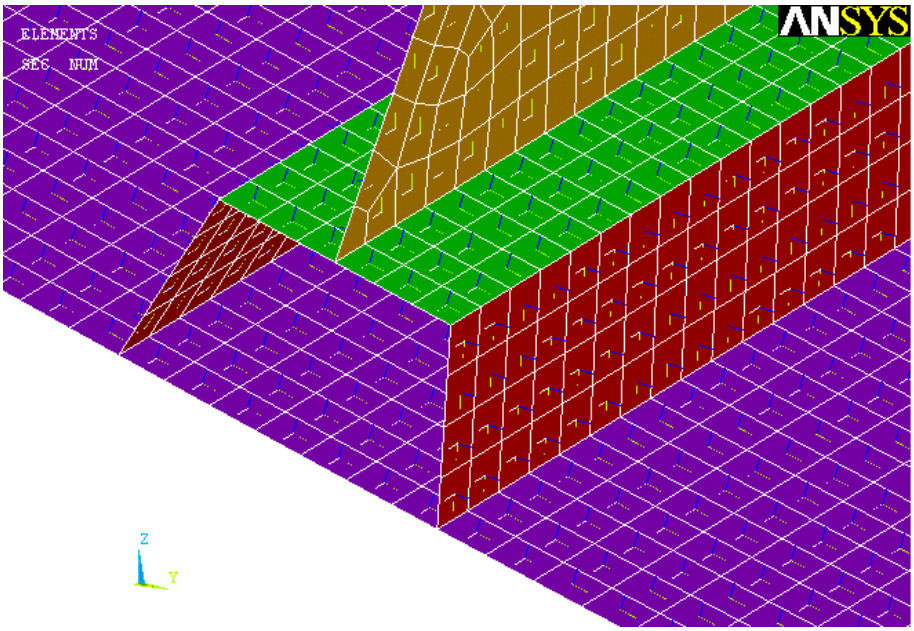

Figure 47. Element local coordinate system – Example 1

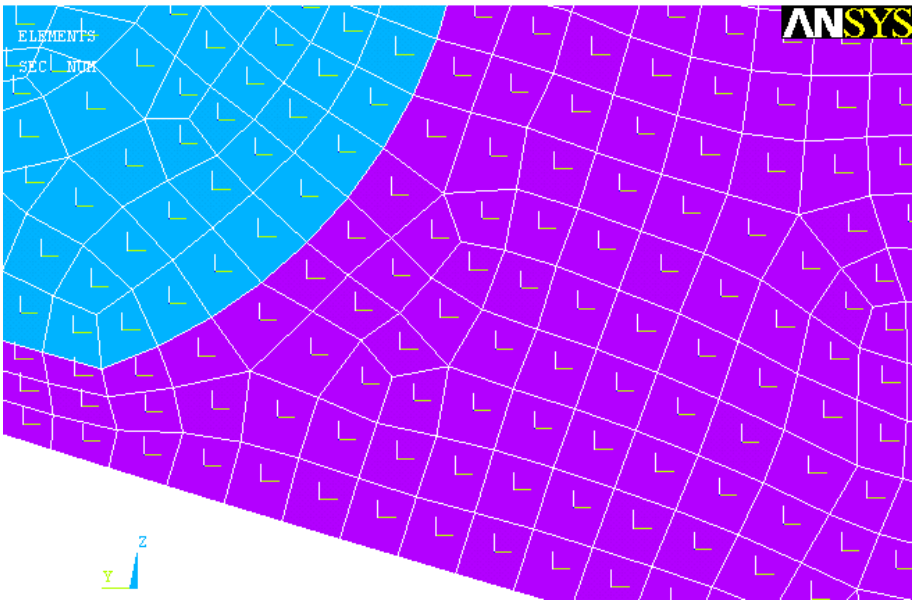

Figure 48. Element local coordinate system - Example 2

The mesh has been checked for faulty elements, i.e. elements not matching the geometrical limits, and after a few iterations was found to be satisfactory.

8.5 BOUNDARY CONDITIONS

Appropriate boundary conditions need to be defined. The boundary condition choice is always and idealization compared to real-life situation, and significantly affects the results.Thus, the results have to be interpreted critically in respect to that boundary conditions imposed on the model, especially close to the boundaries.

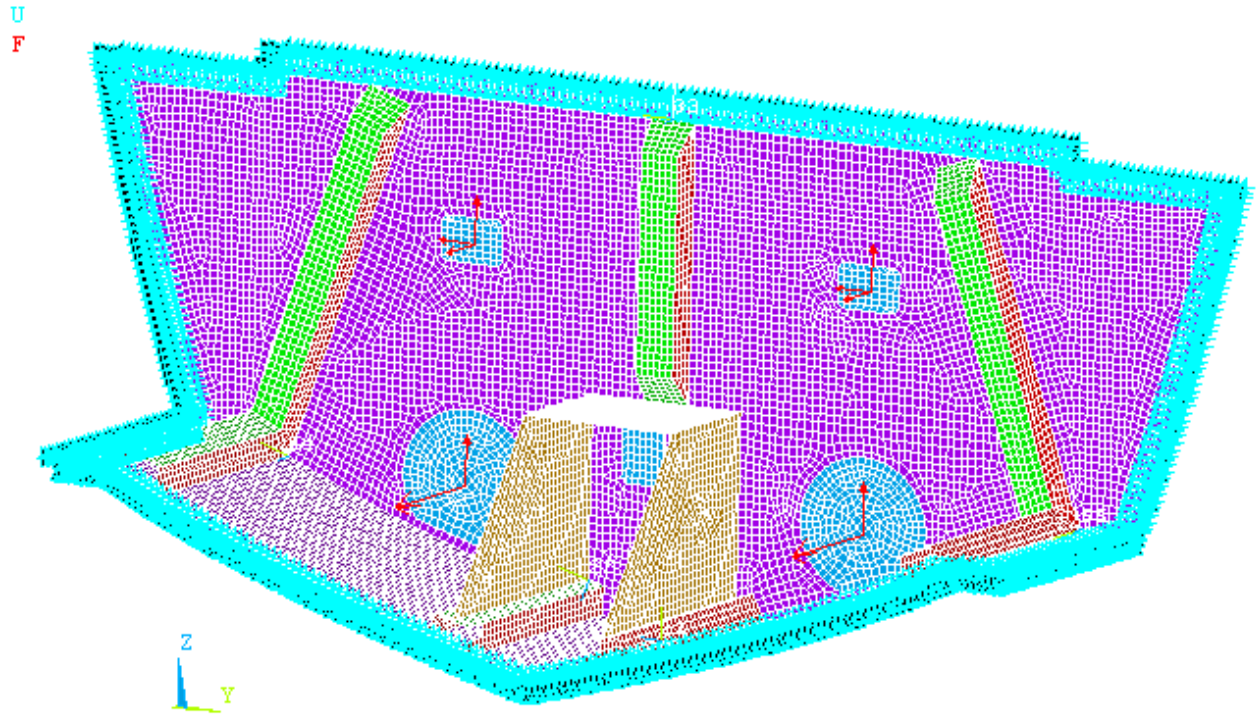

Figure 49. Boundary condition definition

Displacement of nodes has been prohibited in all directions (UX, UY, UZ) all along the edge of the model. Rotation is allowed. It is necessary to take care when interpreting the results close to the edge as they will be greatly affected by the boundary conditions.

8.6 LOADCASE

The loads that the transom will suffer due to the forces exerted on by the SPP drive are provided from the propulsion drive manufacturer. Apart from the trust force, aligned with the axes, significant forces are applied by the hydraulic trim pistons. This loadcase is analogue to full power conditions, with the steering centered.

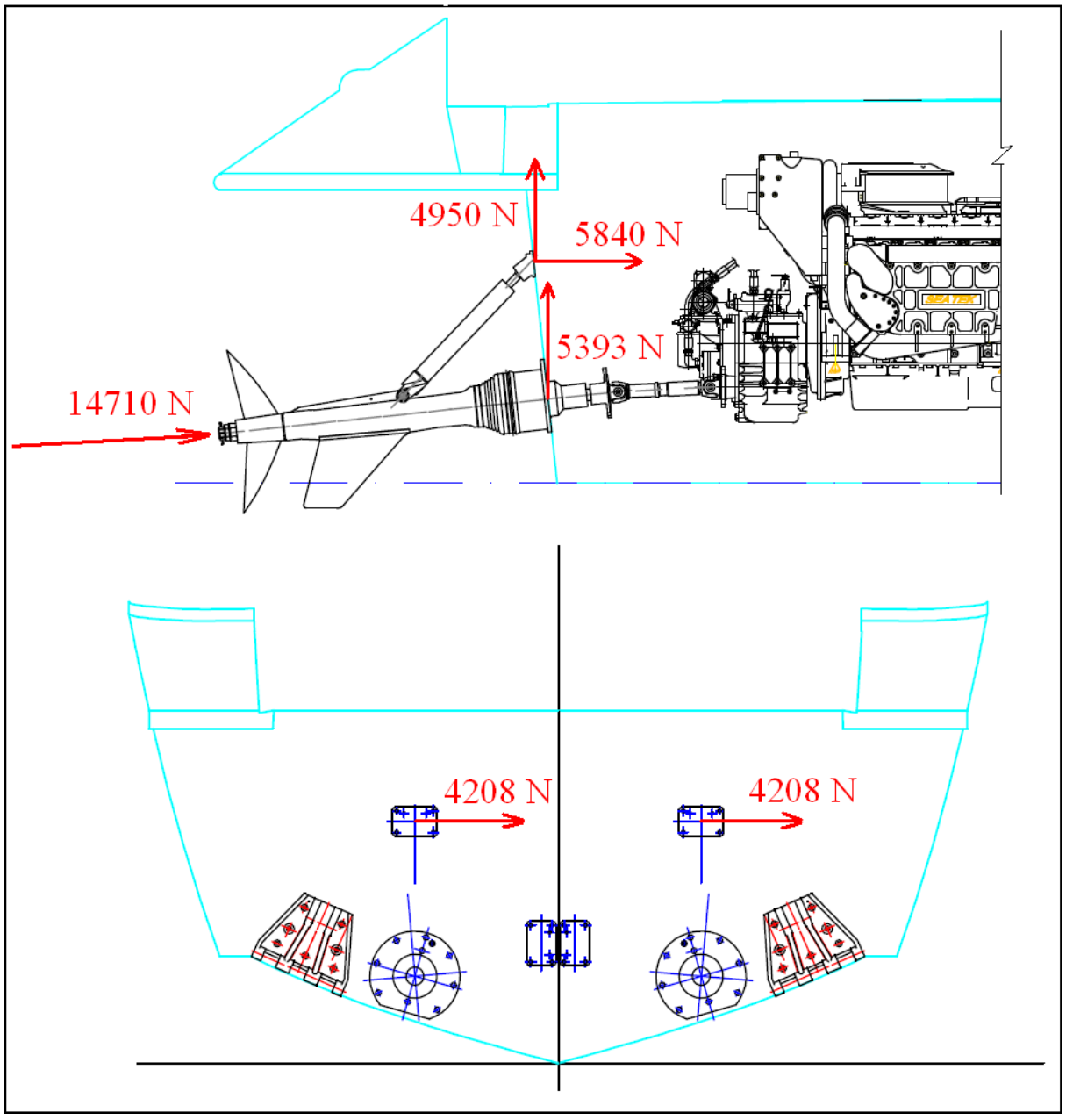

Figure 50. Loads from the SPP drive acting on the transom

While the boat is running, as it is a fast planning hull, the transom is fully ventilated so there are no hydrostatic or hydrodynamic loads expected.

By adding the loads acting on the model node points the problem is fully defined. A linear, static simulation has been performed and a solution has been obtaind.

8.7 POSTPROCESING

8.7.1 Displacements

Post-processing the results implies to display, analyze and interpret the acquired displacements, stress distribution and limits and failure criteria.

The following figure shows the magnitude and distribution of the displacement vector sum:

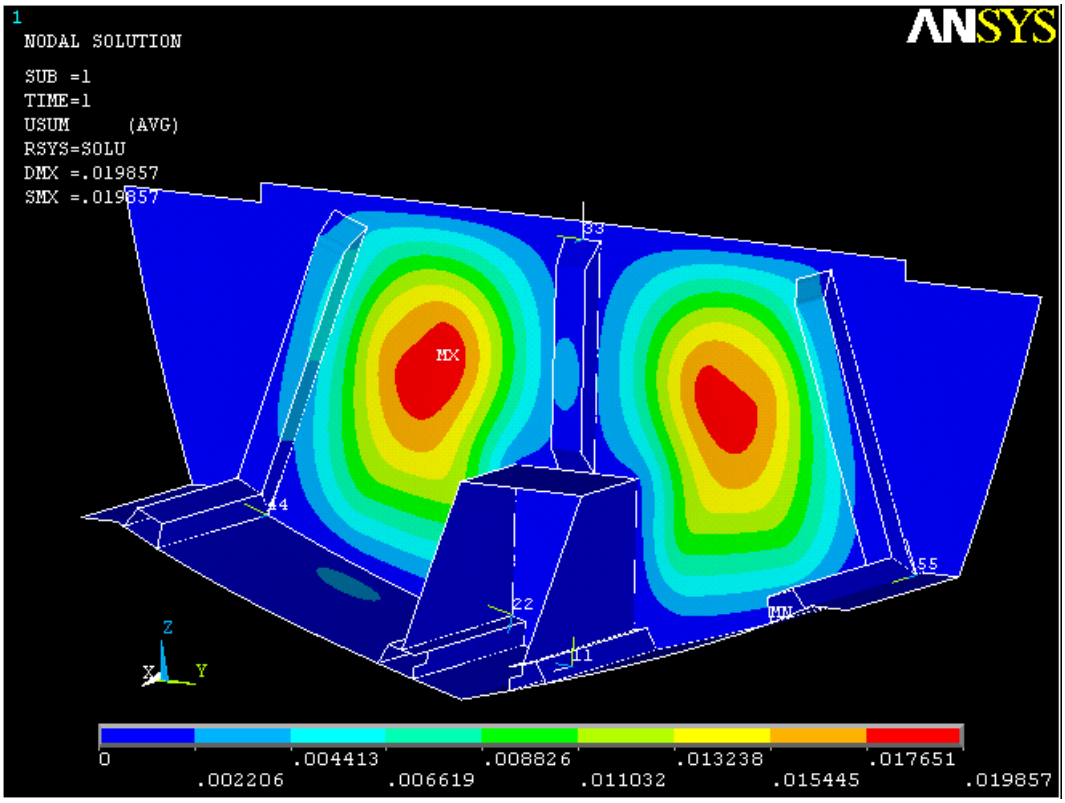

Figure 51. Displacement vector sum

It can be noted that the maximum displacements, for the examined loadcase, are found just below the point where the hydraulic propulsion trim cylinders are attached to the transom. The maximum displacement equals to 19 mm, which is found to be satisfactory.

Further analysis, as the stress distribution and failure criteria, of the composite requires in depth layer per layer approach.

8.7.2 Von Mises Stress

Von Mises stress should not be considered to be a finite design criterion when studying composite layered materials, as it is with isotropic materials. This is due to complex interaction orthotropic effects between the layers of the laminate. Nevertheless it is a good way to understand the stress distribution inside a certain layer.

The following figures will show the Von Mises stress distribution layer per layer. To interpret the results and the magnitude of the stresses it is necessary to remember the section definition, how the materials were laid in each section to be able to understand what each layer globally observed represents.

LAYER 1: Connection plates – Steel

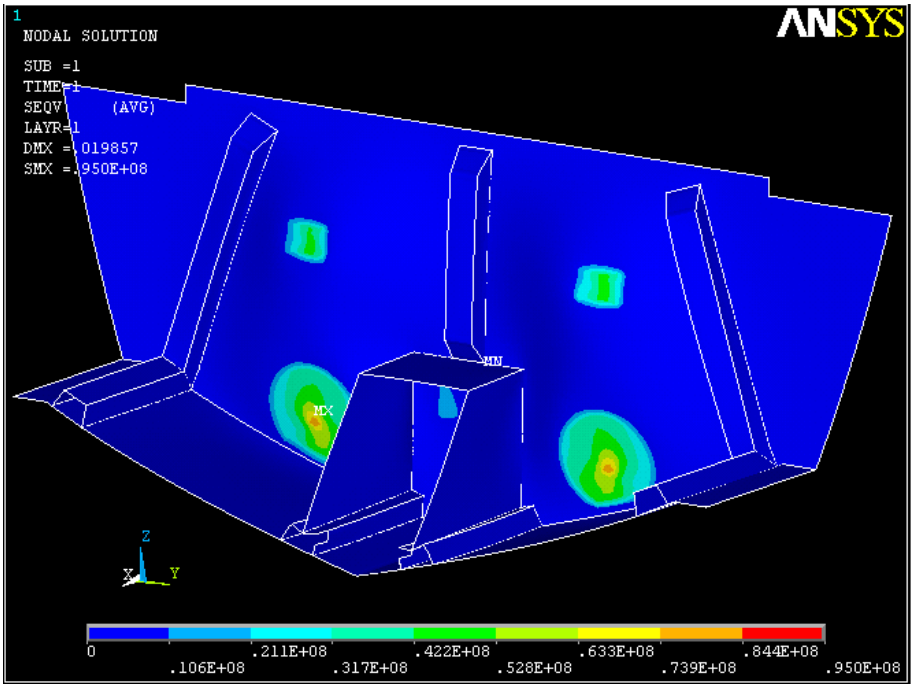

Figure 52.V.M stress distribution in Layer 1 – front veiw

Global deformations of the model are shaded in blue, and the V.M. nodal based contour plot is shown for layer 1 – the connection plates of the SPP drive to the transom strucutre.

LAYER 2: Transom, Bracket, Connections – 0/90 Glass knitted rowing;
Stiffener sides, Stiffener heads – Glass/Carbon Hybrid rowing

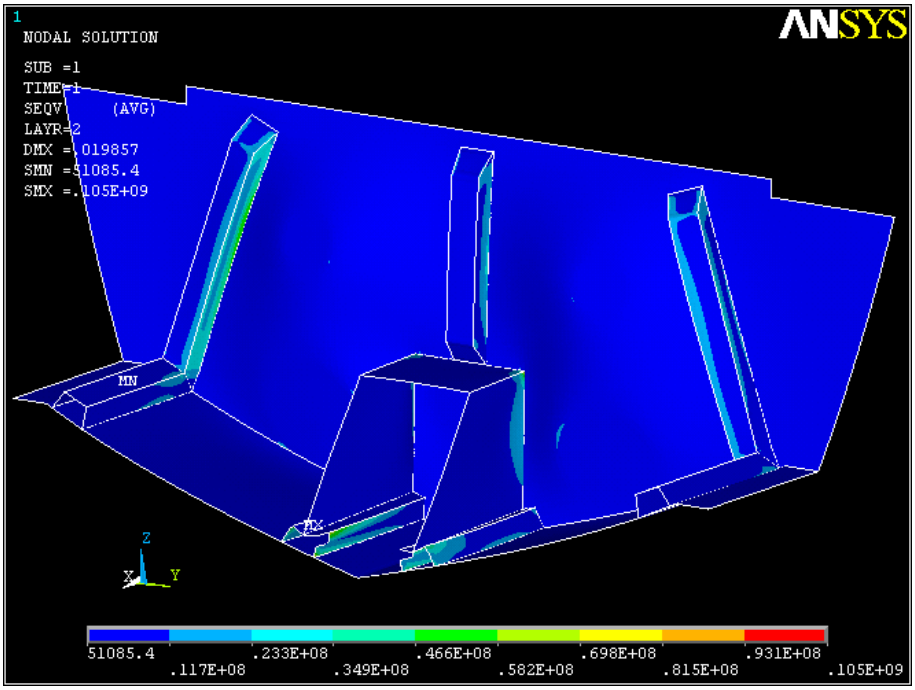

Figure 53.V.M stress distribution in Layer 2 – front veiw

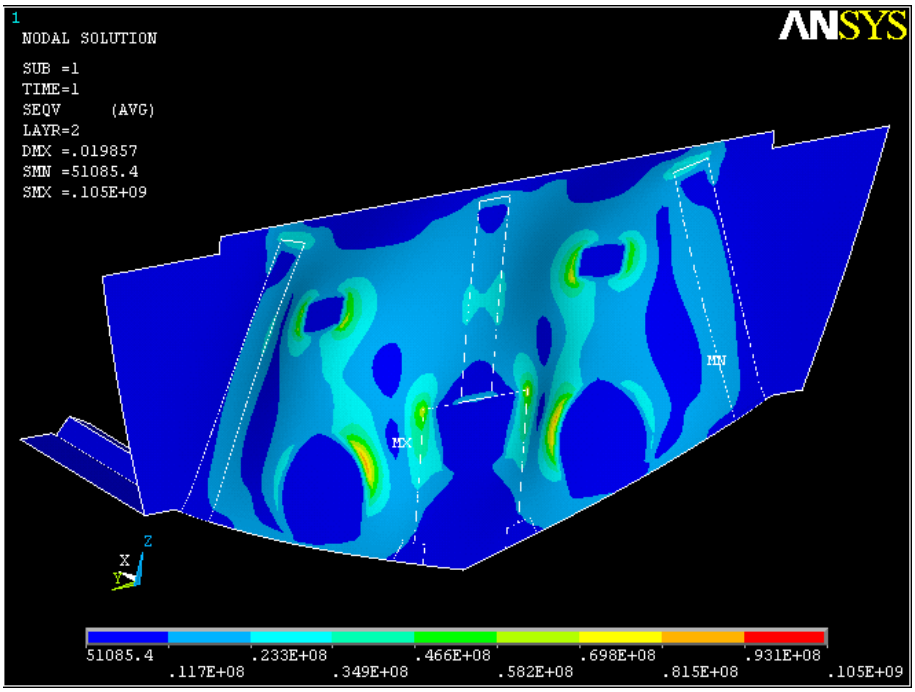

Figure 54. V.M stress distribution in Layer 2 – back veiw

LAYER 3: Transom, Connections – ±45 Glass rowing;
Stiffener head – Unitape carbon

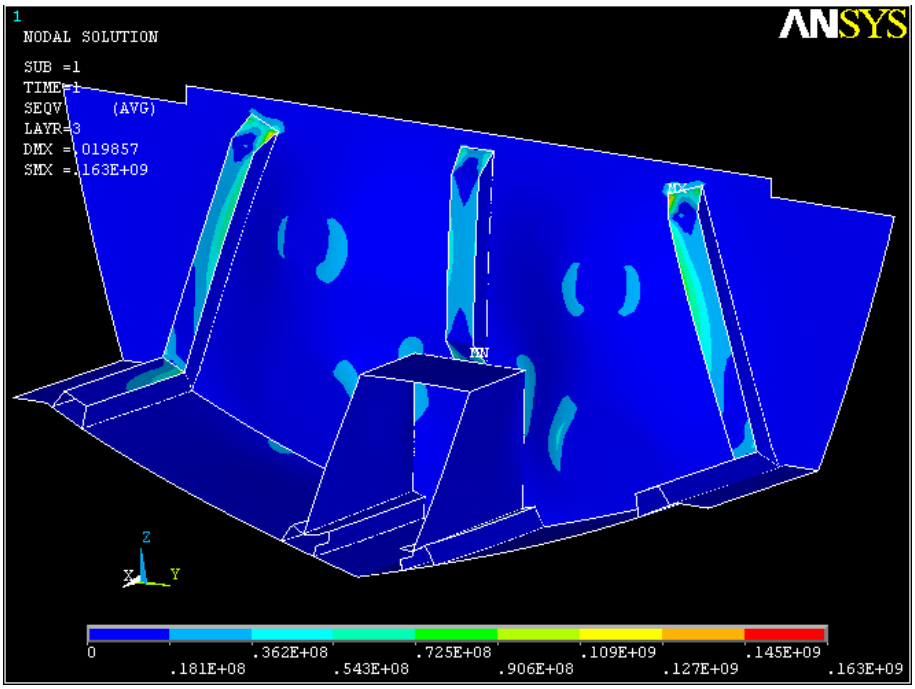

Figure 55.V.M stress distribution in Layer 3 – front view

LAYER 4: Transom, Connections – 0/90 Glass rowing;
Stiffener heads – Glass/Carbon Hybrid rowing

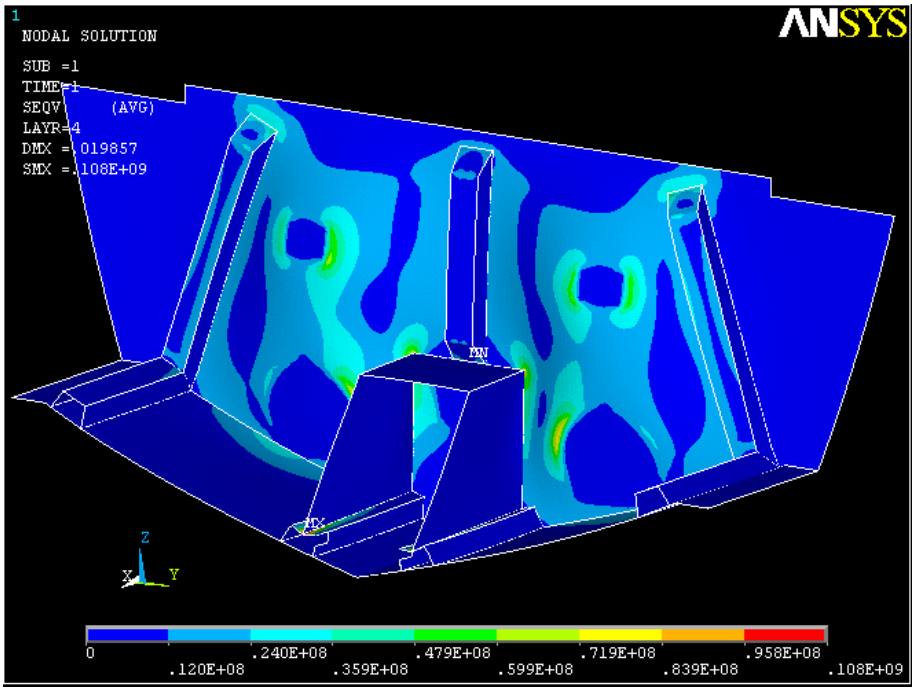

Figure 56.V.M stress distribution in Layer 3 – front view

8.8 FAILURE CRITERIA

Tsai-Wu Strength Index

Strength analysis of composite materials is more complex than that of isotropic materials, due to the orthotropic nature of each ply, and to the many combinations of plies and their interaction with one another across the model. Except in simple cases (e.g. single plies or entirely unidirectional laminates), it is easiest to evaluate the laminate strength using one or more failure theories specific to orthotropic materials.

A long time of research in this area has yielded a multitude of composite failure theories. Some are general and apply to any orthotropic material, while others have specific limitations (e.g. unidirectional only or specific material types). Typical failure theories in many commercial FEA programs include Hill, Hoffman, Tsai-Wu, LaRCO2, Puck, Maximum Stress and Maximum Strain[4].

The Maximum Strain and Maximum Stress theories are termed “non-interactive” since they evaluate the effects of the two orthogonal in-plane principal strains/stresses and the in-plane shear strain/stress in isolation from one another, with failure predicted based on any one of the three exceeding the ply limit for that quantity. While these theories do not accurately predict the failure for multi-axial stress states, they can still help in evaluating principal stress direction; and vectors associated with these constituent stresses can guide in applying reinforcements to best handle areas dominated by highly directional loads.

The Hill, Hoffman, Tsai-Wu, LaRC02 and Puck theories are “interactive” in that they consider together the contributions of the principal and shear strains, with failure predictedbased on a mathematical combination of their effects. Other advanced theories have emerged and are continuing to develop, notably the Multi-Continuum Theory, which can separately predict the failure for the constituent fiber and the matrix (similar to LaRC02, but not restricted to unidirectional plies).

Correctly characterizing the composite materials in the model-building phase and then choosing the proper criteria for evaluating the results are important steps to ensure that the investment in composites FEA yields productive information.
For evaluating the transom model FEA simulation the Tsai-Wu failure criteria has been used. This theory allows nine failure stresses and three additional coupling coefficients.

The governing formulas of the Tsai-Wu failure criteria are:
If the criterion used is the "strength index":

$$\xi_3 = A + B \tag{17}$$

and if the criterion used is the "strength ratio":

$$\xi_3 = 1.0/\left(-\frac{B}{2A} + \sqrt{(B/2A)^2 + 1.0/A}\right) \tag{18}$$

Where:

ξ_3 – value of Tsai-Wu failure criterion

$$A = -\frac{(\sigma_x)^2}{\sigma_{xt}^f \sigma_{xc}^f} - \frac{(\sigma_y)^2}{\sigma_{yt}^f \sigma_{yc}^f} - \frac{(\sigma_z)^2}{\sigma_{zt}^f \sigma_{yc}^f} + \frac{(\sigma_{xy})^2}{\left(\sigma_{xy}^f\right)^2} + \frac{(\sigma_{yz})^2}{\left(\sigma_{yz}^f\right)^2} + \frac{(\sigma_{xz})^2}{\left(\sigma_{xz}^f\right)^2} + \frac{C_{xy}\sigma_x\sigma_y}{\sqrt{\sigma_{xt}^f \sigma_{xc}^f \sigma_{yt}^f \sigma_{yc}^f}} + \frac{C_{yz}\sigma_y\sigma_z}{\sqrt{\sigma_{yt}^f \sigma_{yc}^f \sigma_{zt}^f \sigma_{zc}^f}} + \frac{C_{xz}\sigma_x\sigma_z}{\sqrt{\sigma_{xt}^f \sigma_{xc}^f \sigma_{zt}^f \sigma_{zc}^f}} \tag{19}$$

$$B = \left(\frac{1}{\sigma_{xt}^f} + \frac{1}{\sigma_{xc}^f}\right)\sigma_x + \left(\frac{1}{\sigma_{yt}^f} + \frac{1}{\sigma_{yc}^f}\right)\sigma_y + \left(\frac{1}{\sigma_{zt}^f} + \frac{1}{\sigma_{zc}^f}\right)\sigma_z \tag{20}$$

Cxy,*Cyz*,*Cxz* - *x-y*, *y-z*, *x-z*, respectively, coupling coefficients for Tsai-Wu theory

The Tsai-Wu failure criteria used here are 3-D versions of the failure criterion reported by Tsai and Hahn[8] for the "strength index".
The Tsai-Wu failure index is plotted in the figures. It is a common and generally conservative predictor of ply failure. A failure index is essentially the inverse of a safety factor. A value of

1.0 indicates the onset of first ply failure, with values below 1.0 having a safety margin, and values above 1.0 having failed.

8.8.1 Tsai-Wu F.C results

According to the theory presented above the Tsai-Wu strength index is calculated plotted and examined layer-per-layer.

Layer 1 is an isotropic material (steel) and does not have a failure criterion defined.

Layer 2 failure criterion shows the highest magnitude in the internal sides of the side transom stiffeners, in the glass/carbon hybrid reinforcement layer.

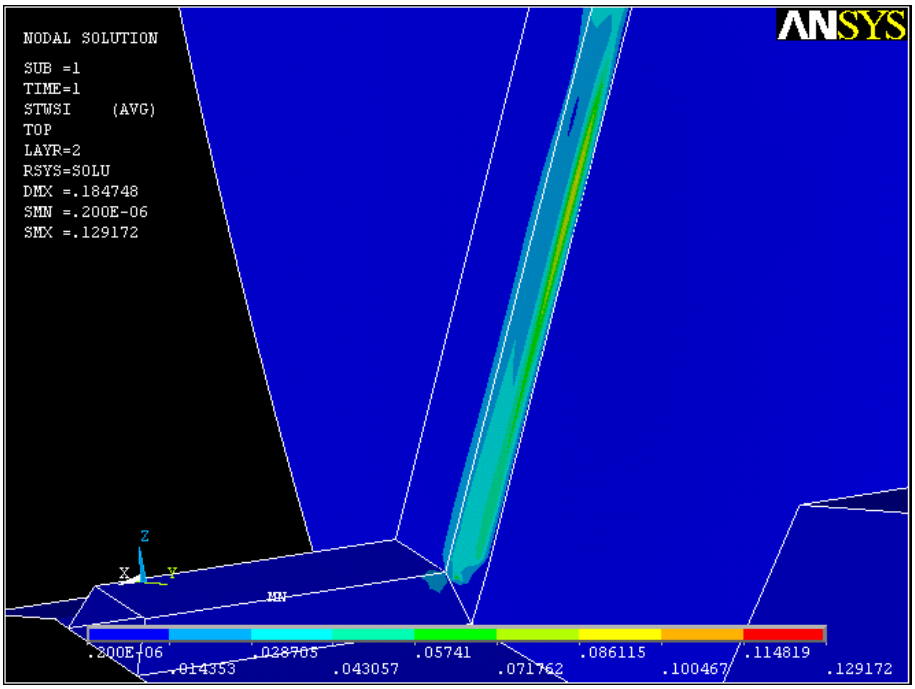

Figure 57. Tsai-Wu strenght index – Layer 2

Maximum value is equal to 0.13, less than 1 (failure limit), and satisfactory.

Layer 3 failure criterion shows the highest magnitude in the lower part of the stiffener head of the side transom stiffeners, in the unitape carbon reinforcement layer.
Maximum value is equal to 0.19, less than 1 (failure limit), and satisfactory.

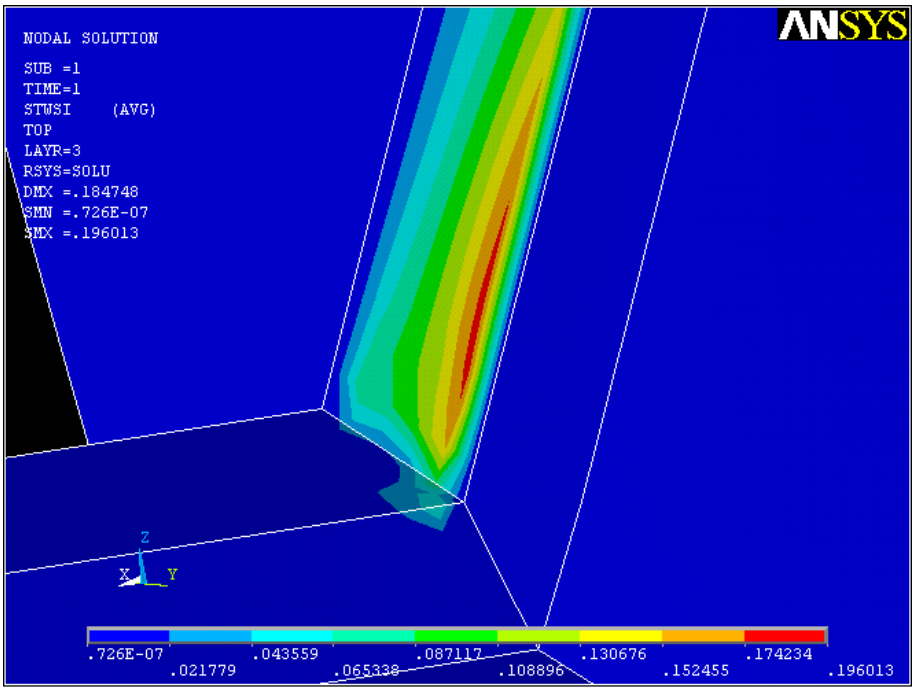

Figure 58.Tsai-Wu strenght index – Layer 3

Layer 4 represents the glass roving reinforcement in the transom and the glass/carbon hybrid reinforcement in the stiffener heads. In the following figure the global distribution is shown.

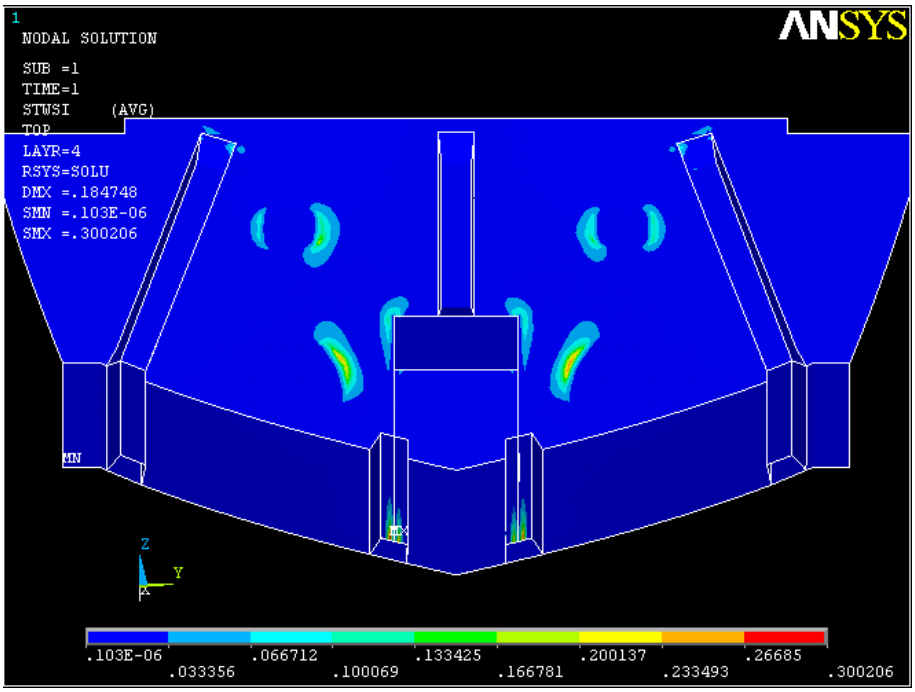

Figure 59.Tsai-Wu strenght index – Layer 4

Maximum value is equal to 0.26, less than 1 (failure limit), and satisfactory. It is found to be on the bottom longitudinal stiffeners where the bracket connects the bottom and the transom.

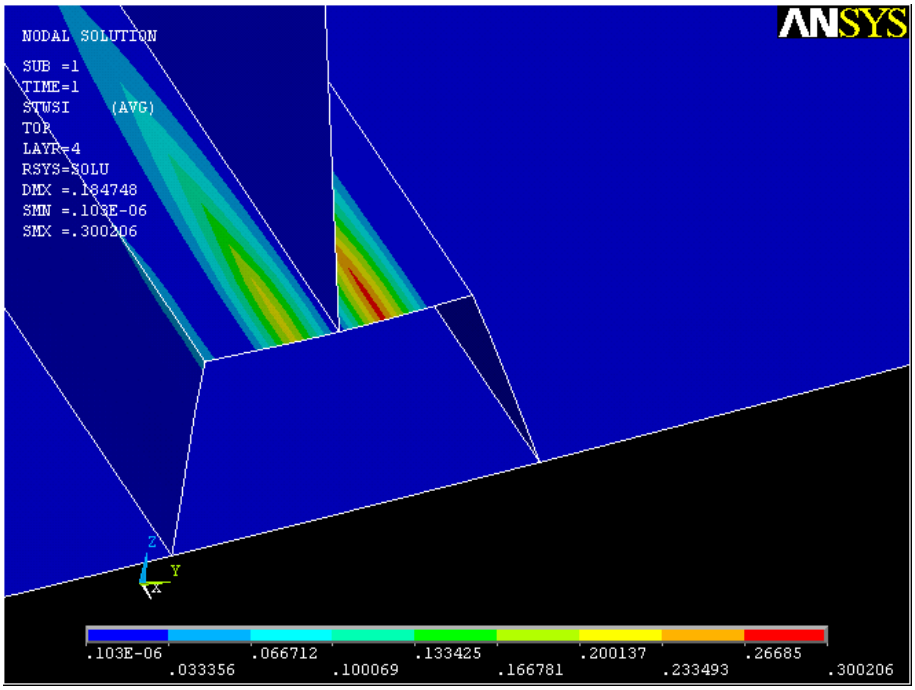

Figure 60.Tsai-Wu strenght index – Layer 4 maximum effect detail

The maximum is found very close to the imposed boundary condition but regarding the fact that the longitudinal stiffeners is attached at that point to a strong transversal stiffener the boundary condition is found to be realistic and the results acceptable.

The results shown in the images reflect the effects of the deflection and stress results from prior images.

Maximum Tsai-Wu strength index found is equal to 0.26 which would in terms of a safety factor be equal to 3.86 and is found to be satisfactory for a part directly analyzed.

9 CONCLUSION

A high speed motor yacht concept has been developed. The yacht is 13.2 meters long ‘open’ type and can reach a top speed of 55 knots. It is driven by two 820 horsepower diesel engines giving power to the Arnesson surface piercing propellers propulsion drive. High top speed of the yacht gives a baseline for its use, aiming at younger clients for weekend cruises, or to be used as a tender next to a larger yacht

The exterior design is defined to give the yacht an aggressive style to be in line with its desired market category, and the general arrangement is made to ensure maximum functionality to four passengers for a one day or a weekend cruise.

A preliminary hydrodynamic calculation, using the Savitsky method has been done to evaluate the resistance of the yacht. It has been noted that the yacht may experience porpoising problem and possible solutions have been given.

Structural design of the hull has been done using the RINA classification code. The hull is made from a vinyl ester composite. Single skin laminate with glass reinforcement is used in the bottom area to absorb the high loads. The sides of the hull are in sandwich construction with glass reinforced skins and balsa core to be lightweight and stiff. Stiffeners have a polyurethane core and are reinforced with hybrid glass-carbon and unidirectional carbon fiber. The lamination scheme and schedule and the dimensions of all parts considered has been verified to satisfy the Rules in an iterative manner.

Structural drawings for hull lamination scheme and schedule and for hull structure have been made and presented.

A detail structural analysis of the transom part was made using ANSYS, a FEA commercial software to evaluate the stresses delivered from the propulsion system. Basic steps of a FEM composite part simulation have been described and shown and the result were found to be satisfactory.

For future work other yacht design areas have to be addressed and then altogether furthermore should be refined following the design spiral to create a competitive project.

10 REFERENCES

[1] – Larsson, L. and Eliasson, R.E., 2007. *Principles of yach Design*, 3rd edition, Camden: International Marine/McGraw-Hill

[2] – RINA Fast Patrol Vessel code, 2007.

[3] – RINA High Speed Craft code, 2002.

[4] – Fornaro, D., 2011. Fine-tuning with FEA. *Professional boatbuilder*, 133, 46.-59.

[5] – Bakker, M.C.M. and Peköz, T., The finite element method for thin-walled members - Basic principles, *Thin-Walled Structures*, 41(2), 179.-189., Elsevier

[6] – ANSYS 13.0 Help // Element Reference // I. Element Library // SHELL181

[7] – Savitsky, D. 1964., Hydrodynamics design of planning hulls, Marine Technology

[8] – Stephen W. Tsai and H. Thomas Hahn. *Introduction to Composite Materials*. Section 7.2. Technomic Publishing Company. 1980.

[9] – RINA, La tecnica dell'infusione nella realizzazione di compositi per la nautical, Linee guida